Zootaxa 4358 (1): 079–106
http://www.mapress.com/j/zt/

Article

ISSN 1175-5326 (print edition)
ZOOTAXA
ISSN 1175-5334 (online edition)

https://doi.org/10.11646/zootaxa.4358.1.3
http://zoobank.org/urn:lsid:zoobank.org:pub:E936B6DF-72C8-4F78-9BB4-99AC1C99C36A

The *Catocala naganoi* species group (Lepidoptera: Noctuidae), with a new species from Vietnam

HUGO L. KONS JR.[1], ROBERT J. BORTH[2], AIDAS SALDAITIS[3, 5] & SERGEI DIDENKO[4]

[1] *719 West Summer Street, Appleton, WI USA. E-mail: hkonsjr@yahoo.com;*
[2] *Lepidoptera Biodiversity, LLC. E-mail: bobborth@sbcglobal.net;*
[3] *Nature Research Centre, Akademijos str. 2, LT-08412 Vilnius-21, Lithuania. E-mail: saldrasa@gmail.com;*
[4] *National University of Science and Technology MISiS, Leninskiy pr. 4, Moscow 119049, Russia. E-mail: sdi13@mail.ru;*
[5] *Corresponding author*

Abstract

The Asian *Catocala naganoi* species group is delimited and reviewed, with a diagnosis of the constituent species based on genitalic, wing pattern, and COI 5' mtDNA characters. The included species are *Catocala naganoi* Sugi, 1982*, C. solntsevi* Sviridov, 1997*, C. naumanni* Sviridov, 1996, and *C. katsumii* **sp. n.** which is described here as new.

Key words: underwing moth*,* new species, mitochondrial DNA, cytochrome oxidase subunit I, Ngoc Linh Mountain

Introduction

Among the Asian *Catocala* Schrank is a small array of medium sized, yellow hindwinged species defined by a number of genitalic and mtDNA characters. These include *C. naganoi* Sugi, 1982*, C. solntsevi* Sviridov, 1997*,* and *C. naumanni* Sviridov, 1996, and we refer to them as the *C. naganoi* species group (the recently described *C. kishidai* Ishizuka*,* 2009 [Figs. 2: J–K] may also be a member of this group as suggested by mtDNA, but *C. kishidai* remains known only from the single female holotype and comparative genitalic data are as yet unavailable). Examples of synapomorphies shared by the three confirmed *naganoi* group species include: diverticulum 2b expanded terminally, and with a distinct notch in the expanded region (Figs. 6: A–H, white arrows); diverticulum 13 large and fairly triangular in shape (dorsal aspect) (Figs. 7: A–F); left and right cucullus unsclerotized except for a prominent patch of sclerotization at the ventral anterior margin fusing with the saccular projection (Figs. 9: A–H & 10: A–H); right lobe of anellus (ventral aspect) with a posterior translucent lightly scerotized membranous extension (Figs. 13: A–H); left lobe of anellus strongly curved posteriorly (rather than anteriorly as in most *Catocala*) (Figs. 11: A–F); and sinus vaginalis expanded and diamond–shaped posterior of lamella antevaginalis (not examined for *C. naumanni*) (Fig. 5: F). This form of diverticulum 2b and the right anellar lobe are as far as known unique to the *C. naganoi* species group. We compared both the morphology and mtDNA of the *C. naganoi* group with most of the other Eurasian *Catocala* species with the hindwing median band fused to the marginal band in two places (in some or all individuals), including: *Catocala hyperconnexa* Sugi, 1965, *Catocala patala* Felder & Rogenhofer, 1874, *Catocala butleri* Leech, 1900, *Catocala formosana* Okano, 1958, *Catocala kuangtungensis* Mell, 1931, *Catocala dejeani* Mell, 1936, *Catocala pataloides* Mell, 1931, *Catocala joyka* Ishizuka, 2006 (male only), and *C. nubilia* Butler, 1881. These species lack all of the aforementioned synapomorphies for the *C. naganoi* species group. Other *Catocala* species for which we examined three dimensional genitalic characters in a broad survey of the genus have at most one of these character states (from apparent independent acquisition), and the closest relatives of the *C. naganoi* group are unclear.

Here we describe another species in the *C. naganoi* species group, based on corresponding morphological and mtDNA characters. This new species occurs in Vietnam, and is allopatric with and sister to the apparent Taiwanese endemic *C. naganoi*.

Accepted by L. Pinheiro: 16 Oct. 2017; published: 28 Nov. 2017

Materials and methods

Genitalia were dissected and imaged by HLK with GT Vision or Automontage imaging systems as described in Kons and Borth (2015). Genitalic terminology follows "Genitalic Structural Terminology for *Catocala* and Related Genera" at http://www.lepidopterabiodiversity.com/Terminology.htm. The 5' region of COI was sequenced by Paul Hebert's lab at the University of Guelph as described in Hebert *et al*. (2003). Sequences were manually aligned in Mesquite version 2.75 (Madison & Madison 2011). Diagnostic combinations of COI 5' characters were identified with the "map characters (show hashmarks)" function of Winclada (Nixon 2002), and haplotypes for characters that vary within the *C. naganoi* species group were identified with the "character diagnoser" function of Winclada. Characters were mapped on the strict consensus of most parsimonious trees (MPTs) for the taxa included in Fig. 16. MPTs were calculated with all four search algorithms at default settings with the best score hit 1,000 times with TNT software (Goloboff *et al.* 2008).

Collection acronyms are as follows: AS = Aidas Saldaitis (Vilnius, Lithuania); HS = Helmut Seibald (Vienna, Austria); KI = Katsumi Ishizuka (Nagano, Japan); MGC = McGuire Center for Lepidoptera Research (Gainesville, FL); NSMT = National Museum of Nature and Science (Tokyo); RJB = Robert J. Borth (Mequon, WI); SD = Sergei Didenko (Moscow, Russia); YPM = Yale Peabody Museum of Natural History (New Haven, CT); ZFMK = Zoologisches Forschungsmuseum, A. Konig (Bonn, Germany).

All specimens examined for this paper are illustrated on the adult plates, with data labels, with the exception of one female *C. pataloides* (dissection No. HLK: 2398, China, Bamianshan, 1800 m, Ruchent side, S–W. Hunnan, June 2005, leg. Wen *et al*. [RJB]).

Catocala katsumii sp. n., Kons, Borth, Saldaitis & Didenko

(Figs. 1: A–G, 3: A–AC, 4: A–F, 5: A–K, 6: A–B, 7: A, 8: A, 9: A–B, 10: A–B, 11: A, 13: A, F, & L, 15: A)

Type material. Holotype: male (Fig. 1: A), DNA voucher No. 22027–150616–VI, Dissection No. HLK:2407, Vietnam, Kon Tum Prov., Ngoc Linh Mountain, vic. N 15.05° W108.02° 1700 m, June 2016 (YPM). **Paratypes:** (Figs. 1:B–G) Vietnam: Kon Tum Prov.: Ngoc Linh Mountain, vic. N 15.05° W108.02° 1700 m: 1 male, Dissection No. HLK: 2409, June 2016 (RJB); 1 female, Dissection No. HLK:2420, June 2016 (RJB); 6 males, June 2016 (RJB); 2 females, June 2016 (RJB); 1 male , DNA voucher No. 22030–150616–VI, May 2015 (RJB); 1 male May 2015, (RJB); 4 males, 6 females, May 2016 (AS, SD); 1 male, 3 females, July 2016 (HS); 1 female, DNA voucher No. 22029–150616–VI, October 2016 (RJB); 3 males, 2 females, December 2016 (RJB). Lào Cai Prov.: 1 female, Dissection No. HLK: 2408, Sapa Mountain, 1600 m, May 2015 (RJB).

Diagnosis. This section allows diagnosis of the four confirmed members of the *C. naganoi species* group. We note that genitalia and COI 5' allow much better delimitation of these species than wing pattern, and we recommend that material from new localities be assessed by genitalia and/or DNA and not solely on wing pattern. Although *C. hyperconnexa* Sugi, 1965 (Figs. 2: L–R) is similar to *C. katsumii* in wing pattern, the genitalic structure of *C. hyperconnexa* is highly divergent and suggests no close relationship with the *C. naganoi* species group (Figs. 9: I, 10: I, 11: G–H, 12: D, 13: I & Q, 14: A–D, & 15: D). *C. pataloides* Mell, 1931 (Figs. 2: S–T) occurs in sympatry with *C. katsumii* and has a similar hindwing to the *C. naganoi* species group, but, as with *C. hyperconnexa*, the divergent genitalia suggest no close relationship (Figs. 9: J, 10: J, 11: I, 12: E & I, 13: J–K, 14: E–I & 15: E). Some additional Asian *Catocala* species have hindwings similar to *C. katsumii* (i.e., median and marginal dorsal hindwing bands doubly connected by black bands along veins Cu2 and 2A) but these are broadly allopatric and again have divergent genitalia (some of these species are compared with the *C. naganoi* species group in supplemental plates available at: http://www.lepidopterabiodiversity.com/SP.htm). Within the *C. naganoi* species group, *C. naganoi* and *C. katsumii* are supported as sister taxa. Examples of synapomorphies include: serrate region present on phallus posterior of ventral hood (Figs. 3: P & 13: B); in ventral aspect the apex of diverticulum 2b projects approximately perpendicular to the base of the phallus hood (Figs. 4: A–B & 18: A, C–D (red arrows)); diverticulum 7.1 present (Figs. 4: A–B & 8: A, C–D); apex of diverticulum 12 curves posteriorly (Figs. 4: A–B & 10: A, C–D (purple arrows)); ventral/posterior surface of diverticulum 7 heavily undulated (Figs. 4: C, E & 8: A, C–D); ventral anterior opening of antrum with roughly symmetrical concave lobes nearly perpendicular to the vertical plane of the antrum; and ventral anterior side of antrum opening nearly as wide as the horizontal width of the antrum (Figs. 5: A & 15: A–B).

Wing Pattern: The maculation of *C. katsumii* is like *C. naganoi,* but the forewings of *C. katsumii* are generally browner and less mottled with white or pale brown, creating a smoother appearance, versus the greyer and coarser appearance of *C. naganoi* (Fig. 1). *C. solntsevi* and *C. naumanni* may have more contrasting darker brown in the basal area (basal to the antemedial line) than in the medial area, whereas in *C. katsumii* there tends to be little contrast between these areas. Some but not all specimens of *C. naganoi, C. solntsevi,* and *C. naumanni* have a variably sized band or patch of contrasting white in the medial area, which is unknown in *C. katsumii*. The ventral wing surfaces separate *C. hyperconnexa* and *C. katsumii*. The basal side of the ventral forewing marginal band is angled in *C. hyperconnexa* (Fig. 2: O) but smooth in *C. katsumii* (Figs. 1: D & G). Both species have a ventral hindwing black streak along vein 2a which extends from the marginal band to the wing base. However, in *C. hyperconnexa* the medial band extends distinctly beyond vein 2A into the anal cell, such that the black streak bisects the medial band (Fig. 2: O). In *C. katsumii* the median band terminates at vein 2A or extends slightly into the anal cell, such that the black streak is fused with the median band terminus creating a non–bisected continuous loop (Figs. 1: D & G). The forewings of *C. hyperconnexa* tend to be coarser and more mottled with white than *C. katsumii,* but are otherwise extremely similar. Some specimens of *C. hyperconnexa* have a contrasting white patch inside the subreniform spot (Figs. 2: L–M) and/or a contrasting whitish band in the median area (Figs. 2: L–N & R), and neither of these conditions has been found in *C. katsumii. C. pataloides* differs from all species in the *C. naganoi* species group by having the dorsal hindwing medial and marginal bands fused or nearly so along vein M2 (Fig. 2: S). The thick black dorsal forewing postmedial line between veins Cu2 and M3 differs from the *C. naganoi* group, where the postmedial line is thick along vein Cu2 and anterior of vein M3, but thin between these veins. Many specimens of *C. pataloides* have a contrasting white patch in the subreniform spot (Fig. 2: S), and we have not seen this in the *C. naganoi* group. It is not clear that *C. solntsevi* and *C. naumanni* can be reliably separated from each other by wing pattern alone (see Remarks; we have found no consistent differences in wing pattern in the limited series we have examined).

Male Genitalia: *C. katsumii* (n=2), *C. naganoi* (n=3), *C. solntsevi* (n=4), *C. naumanni* (n=4 capsule, n=1 vesica).

Vesica (anterior aspect): Inner terminal side of diverticulum 2b (distal of notch dividing sections A and B, demarcated by a white arrow) concave in *C. katsumii* (Figs. 6: A–B) versus convex in *C. naganoi* (Figs. 6: C–D), *C. naumanni* (Fig. 6: E), and *C. solntsevi* (Figs. 6: F–H) (see red arrows). Diverticulum 2b distal of notch globular in *C. katsumii* and *C. naganoi* versus narrower in *C. naumanni* and *C. solntsevi* (Fig. 6). Outer side of diverticulum 1c with at most a shallow concave indentation in *C. katsumii, C. naganoi,* and *C. naumanni,* but with a deep concave indentation in *C. solntsevi* (Fig. 6 (blue arrows)). Outer side of diverticulum 2a and inner side of diverticulum 5 distinctly separated in *C. katsumii* (Figs. 6: A–B), but touching in the other three species (Figs. 6: D–H) (except in one instance where diverticulum 2a slipped over the top of diverticulum 1a during eversion (Fig. 6: C) rather than being forced up closer to diverticulum 5 as in all other preparations in the *C. naganoi* species group). Outer margin of diverticulum 5 with a concave indentation in *C. katsumii* (yellow arrows) but not in the other three species (Fig. 6). Outer side of diverticulum 1a with four distinct lobes in *C. naganoi* (Figs. 6: C–D; lobes designated A–D in blue font), three distinct lobes in *C. katsumii* (Figs. 6: A–B) and *C. solntsevi* (Fig. 6: F), and two distinct lobes in *C. naumanni* (Fig. 6: E).

Vesica (dorsal or ventral aspect): Deep angular separation between diverticula 6 and 6.1 (blue arrows) in *C. naganoi* (Figs. 7: C–D & 8: C–D), whereas only a shallow concave separation in *C. katsumii* (Figs. 7: A & 8: A) and *C. naumanni* (Figs. 7: B & 8: B), and no discernible separation in *C. solntsevi* (Figs. 7: E–F and 8: E–F). Diverticula 9a and 9b both conspicuous in *C. katsumii* (Fig. 7: A), *C. naganoi* (Figs. 7: C–D), and *C. naumanni* (Fig. 7: B) versus 9a indiscernible in *C. solntsevi* (Figs. 7: E–F). Diverticula 9b largest and broadest in *C. naumanni* (Figs. 7: B & 8: B), similar in *C. katsumii* and *C. naganoi* (Figs. 7: A, C–D & 8: A, C–D), but more elongate in *C. solntsevi* (Figs. 7: E–F & 8: E–F).

Vesica (dorsal aspect, phallus hood behind image): Base of outer side of diverticulum 13 (left purple arrow) arising from outer edge of diverticulum 10 in *C. katsumii* (Fig. 7: A) and *C. naumanni* (Fig. 7: B) versus rising from the interior of diverticulum 10 in *C. naganoi* (Figs. 7: C–D) and *C. solntsevi* (Figs. 7: E–F). Diverticulum 7 small and not extending dorsally over the vesica in *C. naumanni* (Fig. 7: B) versus prominent and extending dorsally over the vesica in the other species (Figs. 7: A, C–F). Deep separation between diverticula 6 and 7 (green arrows) in *C. katsumii* (Fig. 7: A) and *C. naganoi* (Figs. 7: C–D) versus shallow separation in *C. naumanni* (Fig. 7: B) and *C. solntsevi* (Figs. 7: E–F).

FIGURE 1. Imagos of *C. katsumii, C. naganoi,* & *C. solntsevi*.

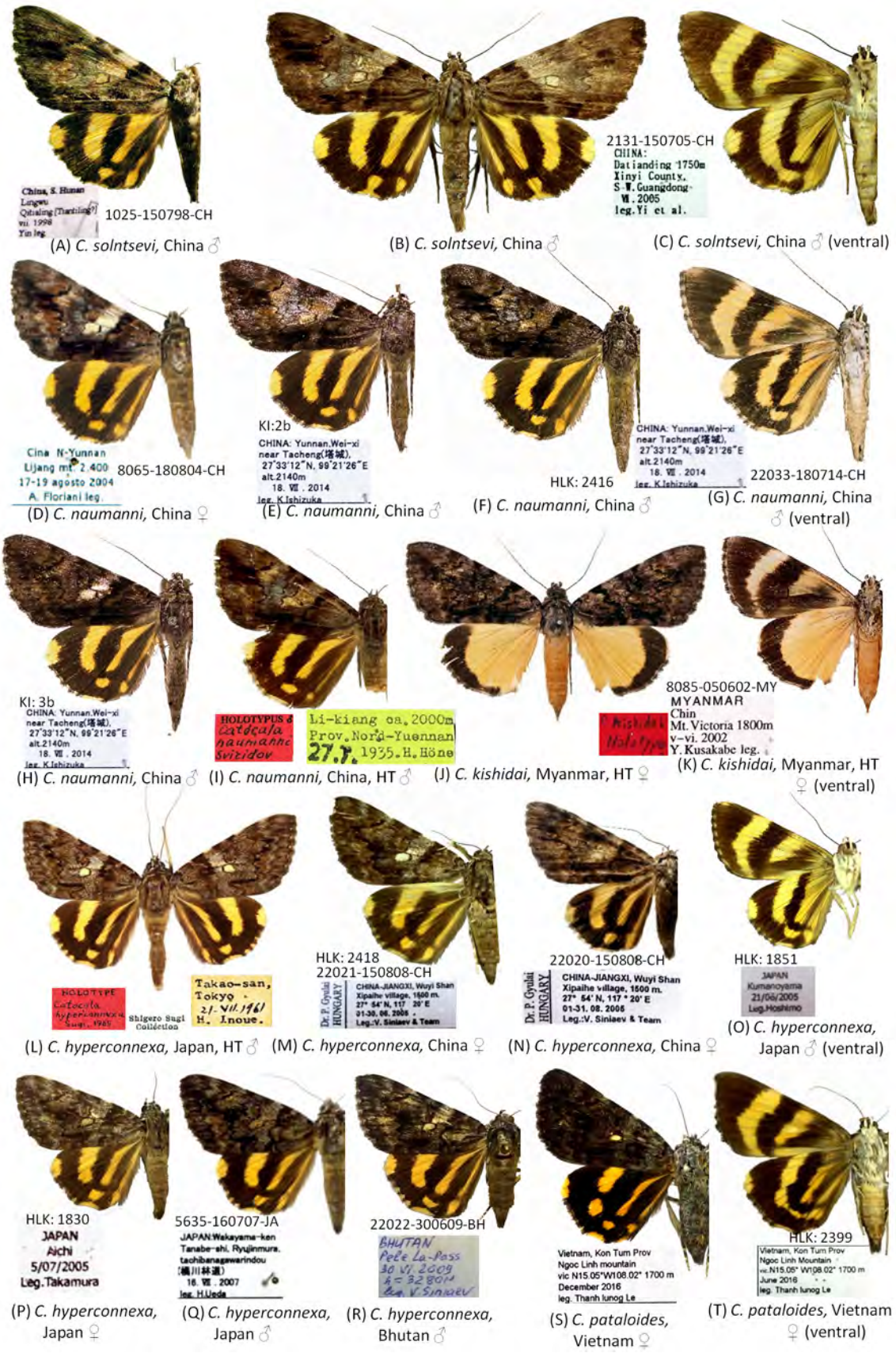

FIGURE 2. Imagos of *C. solntsevi*, *C. naumanni, C. kishidai*, *C. hyperconnexa* and *C. pataloides*.

FIGURE 3. Male genitalia and leg structures of the *C. katsumii* holotype.

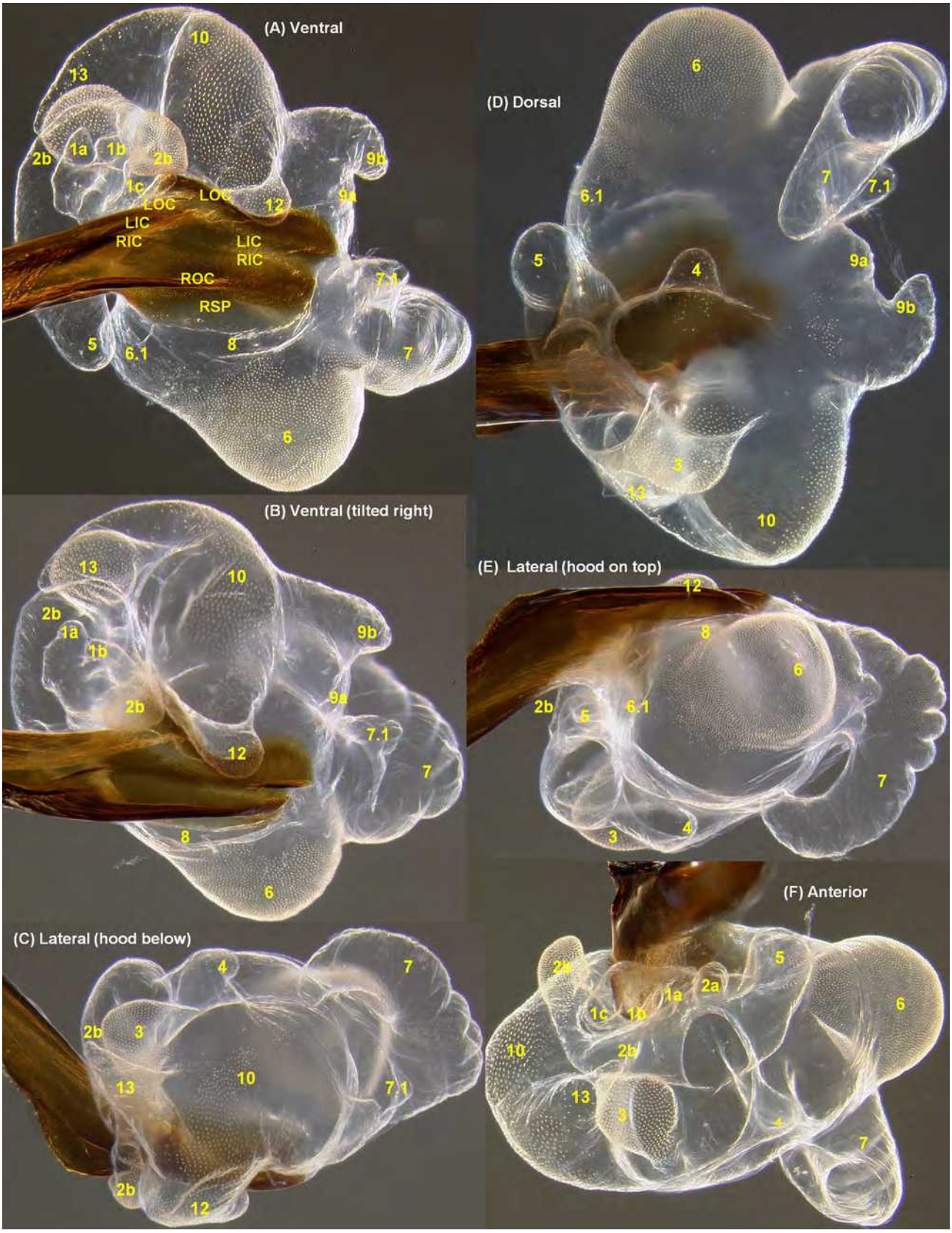

FIGURE 4. Three dimensional vesica structure of the *C. katsumii* holotype.

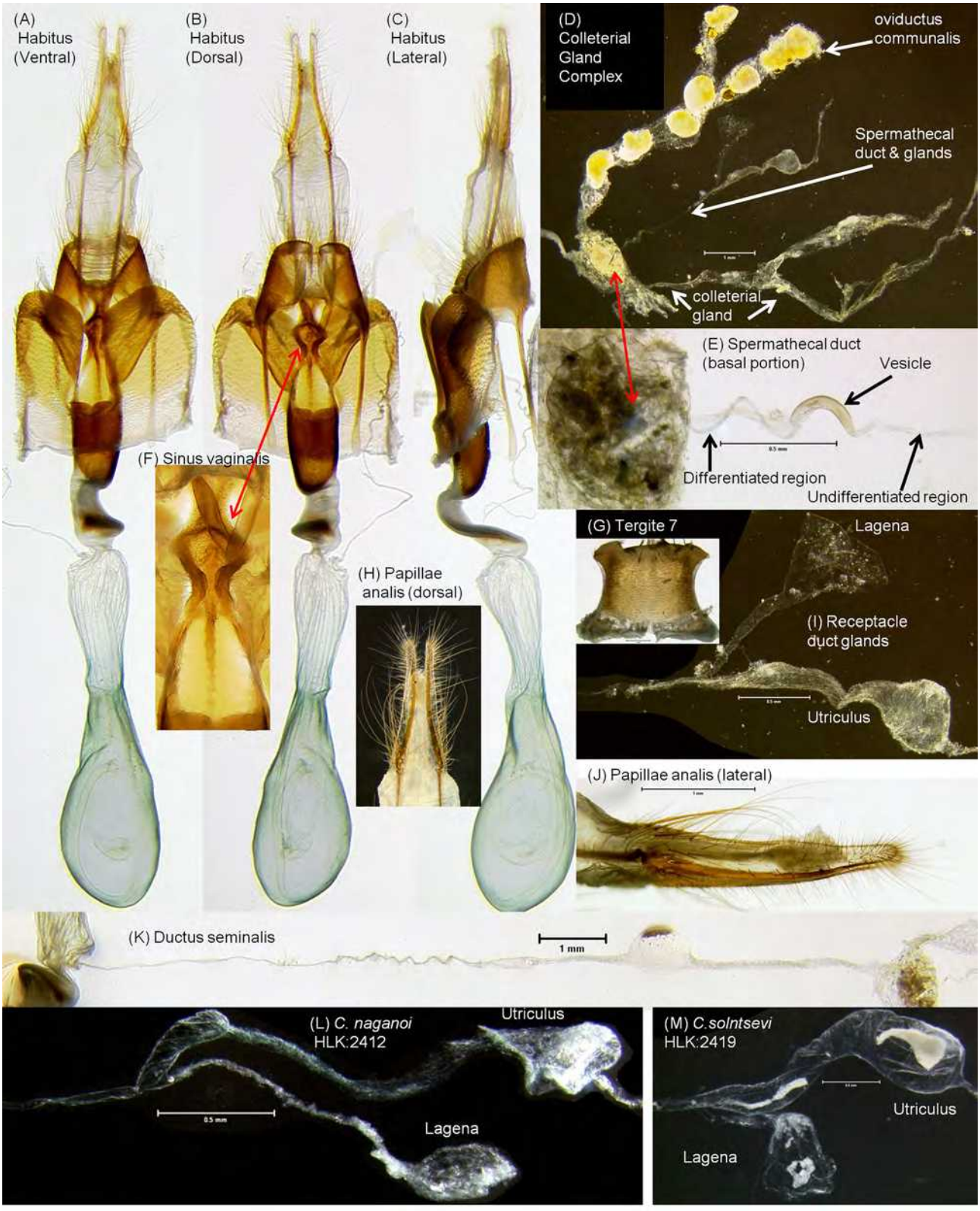

FIGURE 5. Female genitalic structures of *C. katsumii*.

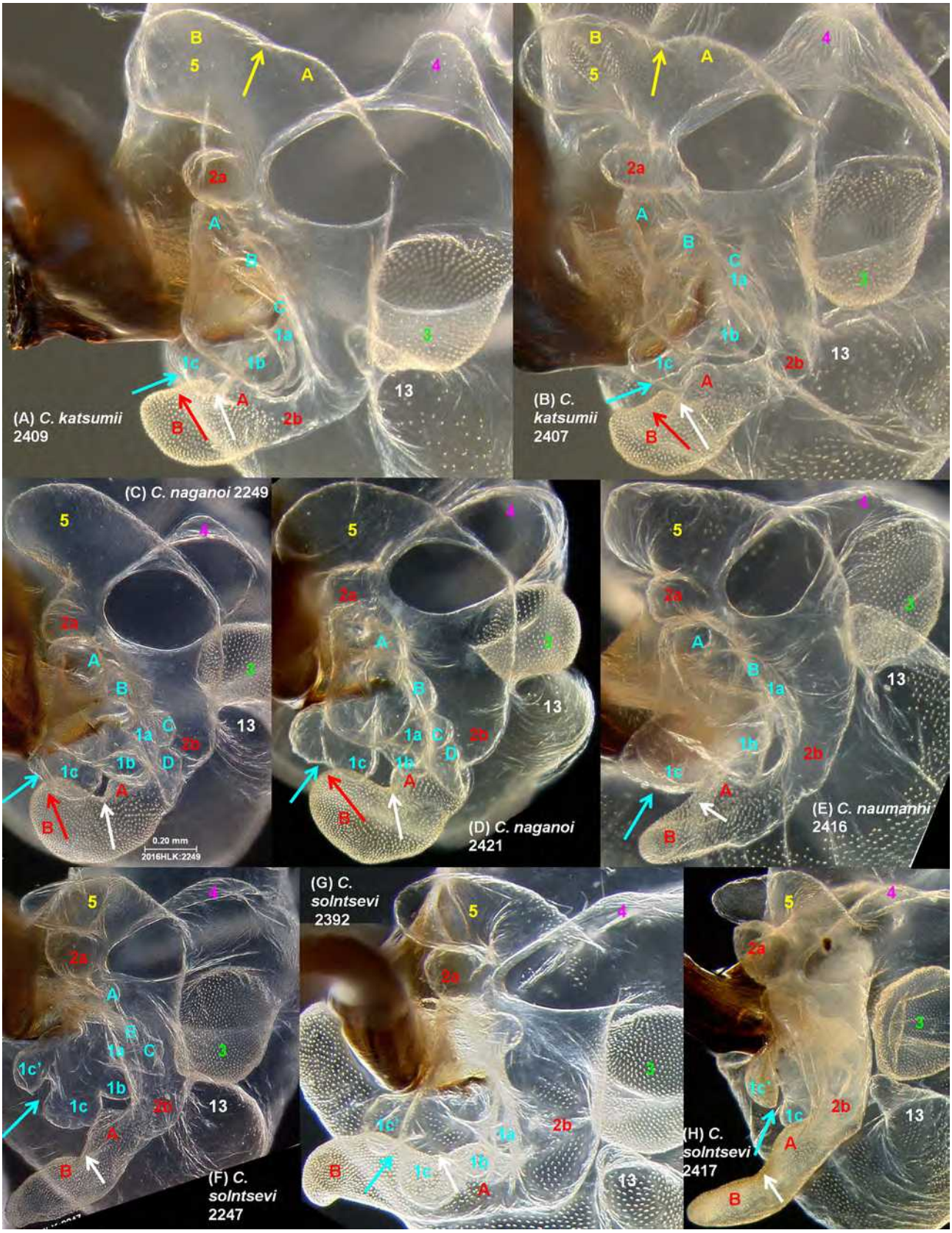

FIGURE 6. Diagnostic vesica characters between *C. katsumii, C. naganoi, C. naumanni,* and *C. solntsevi* (part); anterior aspect zoomed in on the anterior rosette of diverticula 2–5 and diverticulum 1.

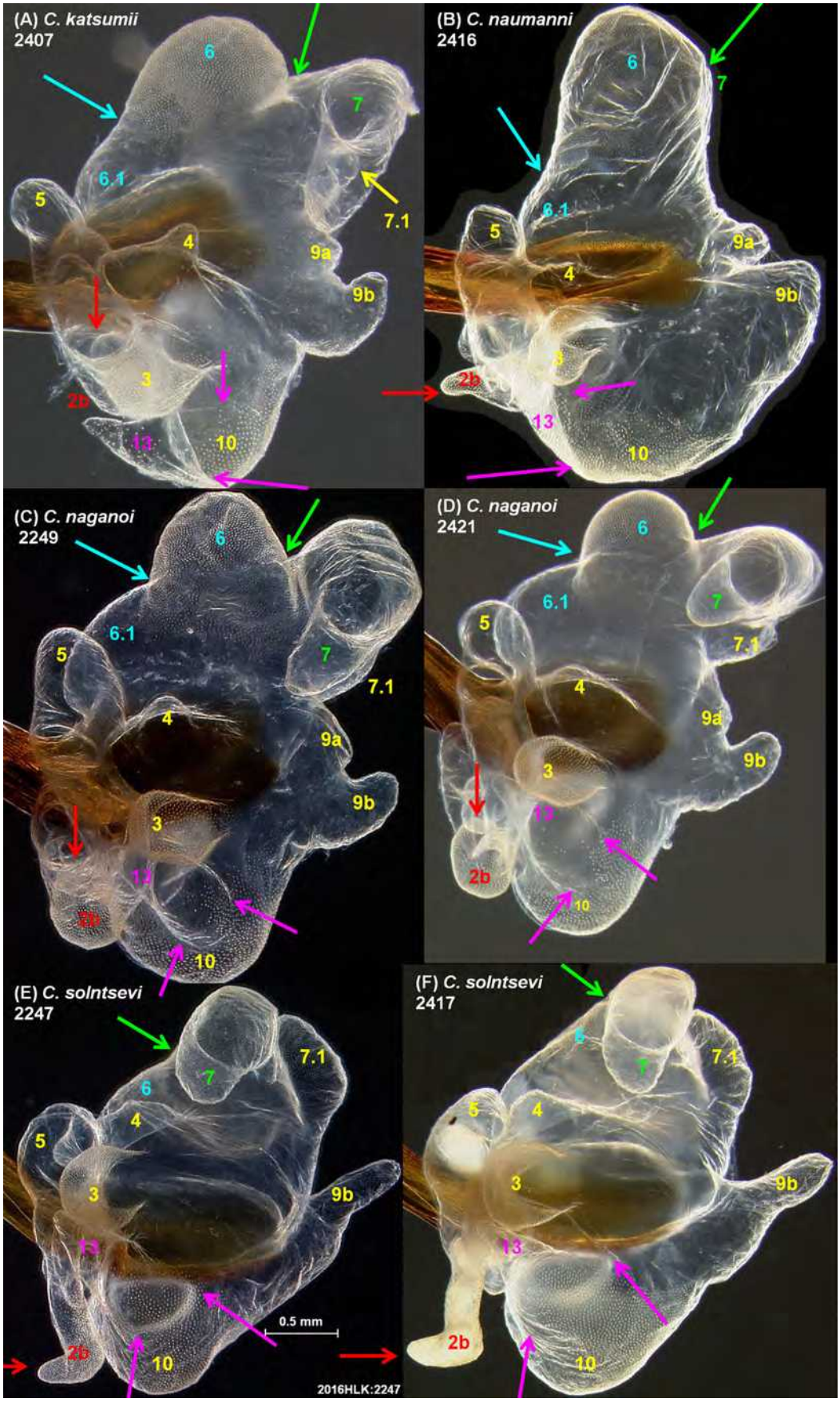

FIGURE 7. Diagnostic vesica characters between *C. katsumii, C. naganoi, C. naumanni,* and *C. solntsevi* (part); dorsal aspect (opposite posterior phallus hood).

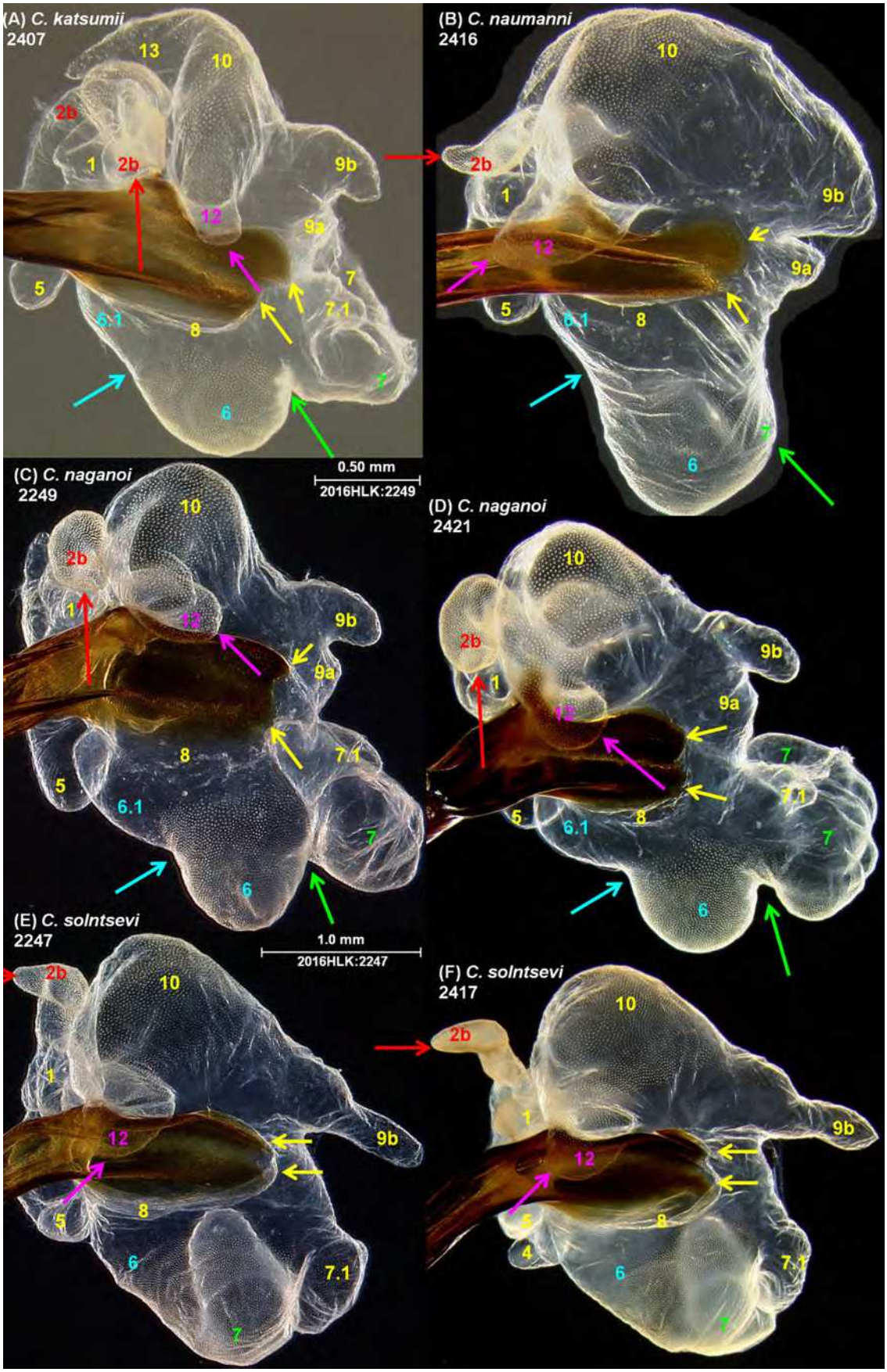

FIGURE 8. Diagnostic vesica characters between *C. katsumii, C. naganoi, C. naumanni,* and *C. solntsevi* (part); ventral aspect (posterior phallus hood in front).

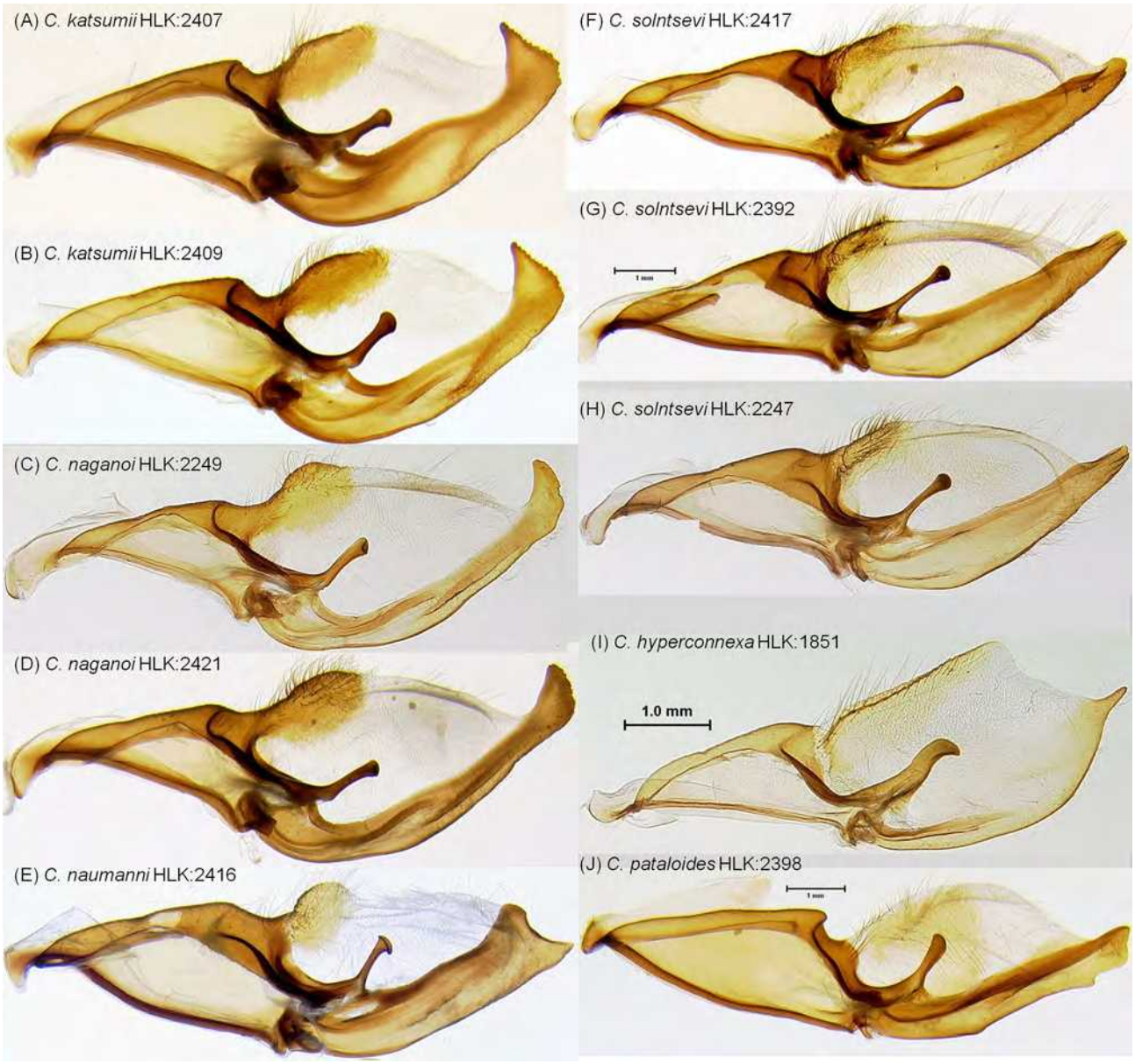

FIGURE 9. Comparison of the left valva (inner side, ventral edge on top) between six *Catocala* species.

Vesica (ventral aspect, phallus posterior hood in front of image): Apex of diverticulum 2b (red arrows) projects approximately perpendicular to the posterior phallus hood in *C. katsumii* (Fig. 8: A) and *C. naganoi* (Figs. 8: C–D) versus approximately parallel in *C. naumanni* (Fig. 8: B) and *C. solntsevi* (Figs. 8: E–F). Diverticulum 7.1 indiscernible in *C. naumanni* (Fig. 8: B), versus present and conspicuous in the other species (Figs. 8: A, C–F). Apex of diverticulum 12 (purple arrows) projects posteriorly–inward in *C. katsumii* (Fig. 8: A) and *C. naganoi* (Figs. 8: E–F) versus anteriorly–inward in *C. naumanni* (Fig. 8: B) and *C. solntsevi* (Figs. 8: E–F). Posterior side of diverticulum 7 strongly undulated in *C. katsumii* and *C. naganoi* (most clearly seen in lateral aspect (Figs. 4: E–C), but also clear in ventral aspect (Figs. 8: A, C–D), much more weakly undulated in *C. solntsevi* (Figs. 8: E–F), and not discernibly undulated in *C. naumanni* (Fig. 8: B).

Valvae: While the apex of valvae costa can be highly variable infraspecifically in *Catocala* species where it extends posteriorly beyond the cucullus, there are some differences within the *naganoi* species group that we observed to be consistent within all of the species among the series examined. Left valva costal apex tapering and narrowly rounded in *C. solntsevi* (Figs. 9: F–H) versus widening in the other three species (Figs. 9: A–E). The ventral corner of the flared left costal apex tapers to a point in *C. katsumii* (Figs. 9: A–B) whereas it is more smoothly rounded in *C. naganoi* (Figs. 9: C–D) and *C. naumanni* (Fig. 9: E). The dorsal corner of the flared left

costal apex tapers to a point in *C. naumanni* (Fig. 9: E), but is irregularly rounded in *C. katsumii* (Figs. 9: A–B) and *C. naganoi* (Figs. 9: C–D). The width of the left valve costa between the clasper base and the posterior edge of the cucullus is distinctly narrower in *C. naganoi* than in the other three species (Fig. 9). The left clasper curves inward to the least extent in *C. solntsevi* such that it appears the longest in inner aspect (Figs. 9: F–H); it curves inward to the greatest extent in *C. naumanni* and projects posteriorly to the least extent (Fig. 9: E). In *C. solntsevi* the left costa is widest across from the clasper shaft and narrows anterior and posterior of this point, whereas in the other three species the costa is wider at the base of the clasper, constricts posteriorly across from the clasper shaft, then widens posteriorly beyond the clasper, constricts again, and finally widens again apically (Fig. 9). Right clasper narrower in *C. naumanni* (Fig. 10: E) and *C. solntsevi* (Figs. 10: F–H) than for *C. katsumii* (Figs. 10: A–B) and *C. naganoi* (Figs. 10: C–D). Sclerotized area in ventral anterior corner of right cucullus borders a distinct ventral lobe in *C. katsumii, C. naganoi,* and *C. naumanni,* whereas the ventral edge of the cucullus is smooth at the border of the membranous and sclerotized areas in *C. solntsevi* (Fig. 10).

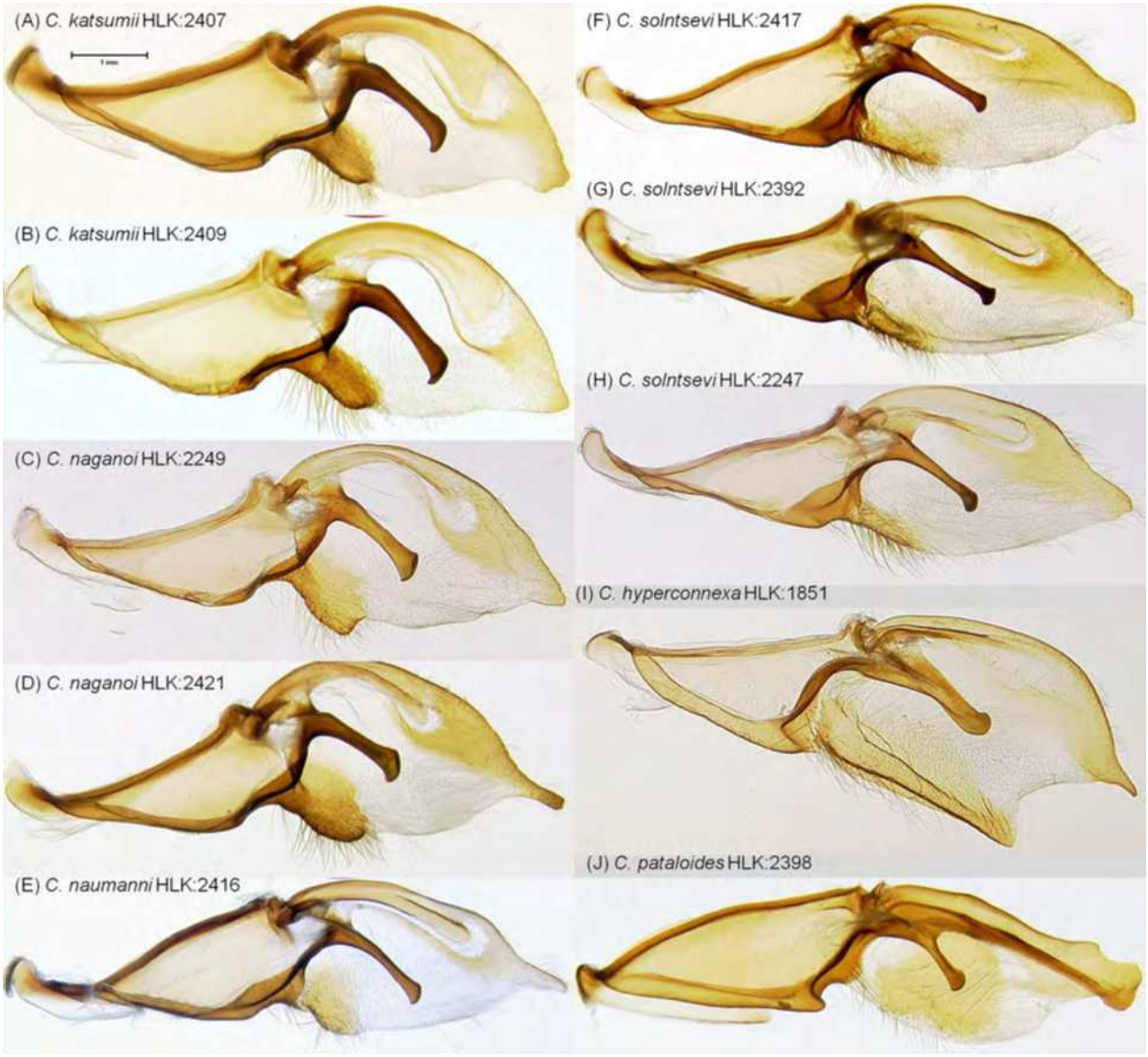

FIGURE 10. Comparison of the right valva (inner side, ventral edge on bottom) between six *Catocala* species.

Juxta/Anellus (Figs. 3 L & 11): The posterior left side of the anellus has a sharp angular bend (slightly obtuse to nearly 90 degrees) in *C. katsumii, C. naganoi,* and *C. naumanni* whereas this area is broadly concave in *C. solntsevi*. The apex of the left anellus lobe abruptly narrows apically (due to a strong bend on the anterior side) in *C. solntsevi* and *C. naumanni*, versus a much more progressive tapering in *C. katsumii* and *C. naganoi*. The anellus is similar and not clearly diagnosable between *C. katsumii* and *C. naganoi*. The posterior outer apex of the juxta is

less narrowly fused with the anellus in *C. katsumii* and *C. naganoi* versus *C. naumanni* and *C. solntsevi,* such that when the juxta/anellus is flattened out the juxta lobes form an obtuse angle in *C. katsumii* and *C. naganoi* but an acute angle in *C. naumanni* and *C. solntsevi.*

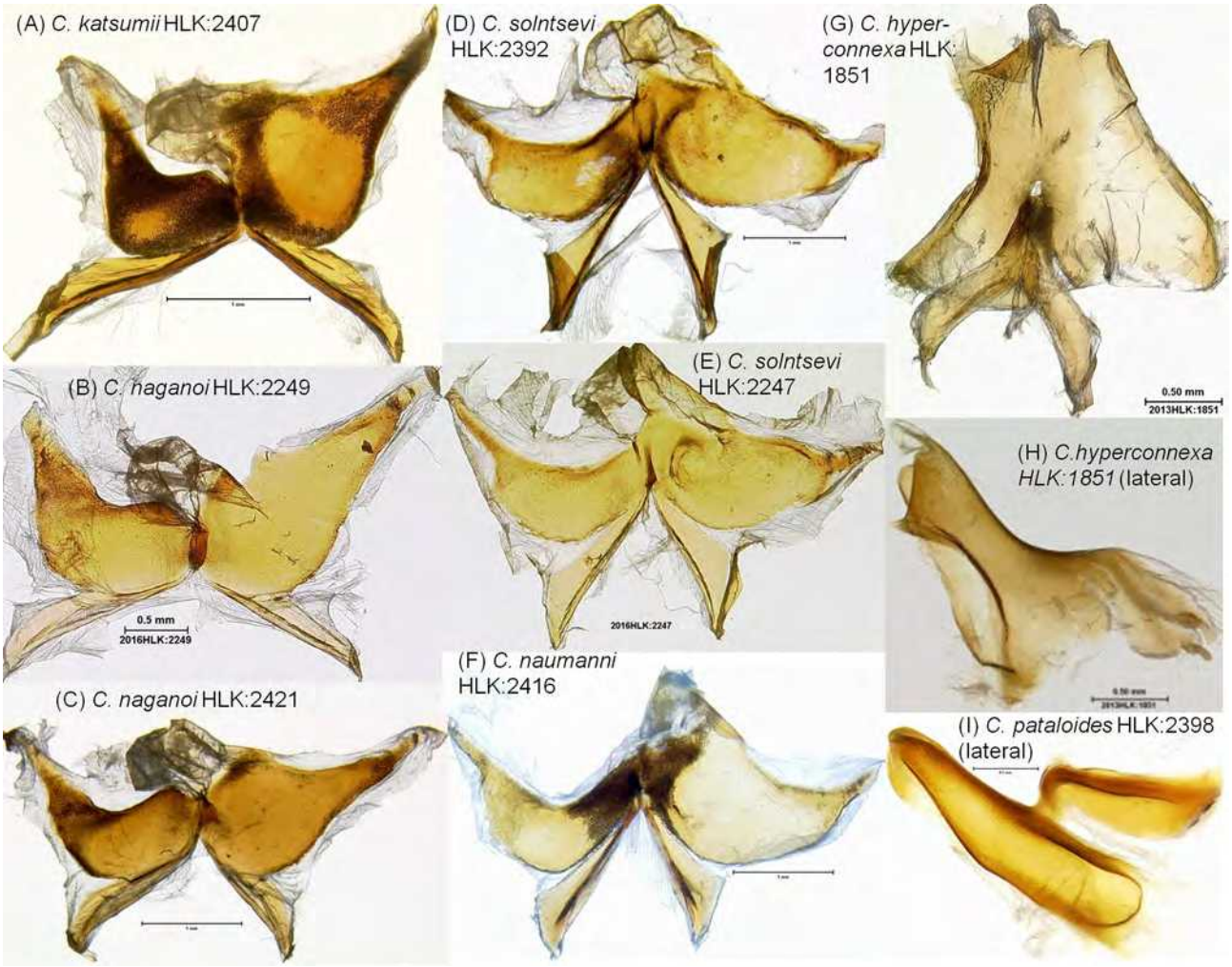

FIGURE 11. Comparison of the juxta and anellus between six *Catocala* species (ventral and flattened on slide unless designated "lateral").

Phallus: In all four species the apex of the posterior phallus hood is divided into two lobes (yellow arrows) divided by a concave gouge; however, the left lobe extends distinctly farther posteriorly than the right lobe in *C. katsumii* (Figs. 4: A & 8: A) and *C. naumanni* (Fig. 8: B) versus both lobes extending a comparable distance posteriorly in *C. naganoi* (Figs. 8: C–D) and *C. solntsevi* (Figs. 8: E–F). In *C. katsumii* and *C. naganoi* the subapical ventral side of the phallus has a serrate keel covered with minute spines (Figs. 3: P & 13: B), whereas this area has a single much larger quadrate tooth in *C. naumanni* (Fig. 15: H) but is smooth in *C. solntsevi* (Figs. 15: D–E). The phallus of all of these species is curved in three dimensions and apparent shape vary greatly between different orientations of the same individual specimen. However, when viewed from comparable orientations, such as with the coecum opening oriented laterally and on top (Figs. 3: P & 15: A–E) or face on (Figs. 3: N & 15: F–H) *C. katsumii* and *C. naganoi* are similar in shape (any possible differences between these two species are too small to detect above apparent differences that result from not being able to align different individuals in exactly the same orientation); however, *C. naumanni* and *C. solntsevi* each have unique and distinctive shapes within this group.

Female Genitalia: *C. katsumii* (n=2), *C. naganoi* (n=2), *C. solntsevi* (n=2), *C. naumanni* (not studied). The anterior margin of the antrum opening has two shallow convex lobes in *C. katsumii* (Fig. 5: A) and *C. naganoi* with a small medial triangular depression, whereas in *C. solntsevi* the entire anterior margin is triangular shaped. The opening is also much wider anteriorly in *C. katsumii* and *C. naganoi* than in *C. solntsevi*. The anterior margin of the lobes of the lamella antevaginalis are concave in *C. katsumii* (Fig. 5: A), convex in *C. naganoi,* and convex with a

small concave depression on the inner side in *C. solntsevi* (Fig. 15, red arrows). The sides of the antrum are asymmetric in *C. katsumii* and *C. naganoi* but symmetric in *C. solntsevi*. In *C. solntsevi* both sides the antrum strongly taper anteriorly for over 2/3 of their length, whereas in *C. katsumii* and *C. naganoi* the left side (ventral aspect) strongly tapers in the posterior third of the antrum length. The lagena is shaped like an inverted triangle in *C. katsumii* (Fig. 5: I), ovuloid in *C. naganoi* (Fig. 5: L), and irregular in *C. solntsevi* (Fig. 5: M). The utriculus and stalk of the lagena is distinctly longer in *C. naganoi* (Fig. 5: L) than in the other two species (Figs. 5: I & M).

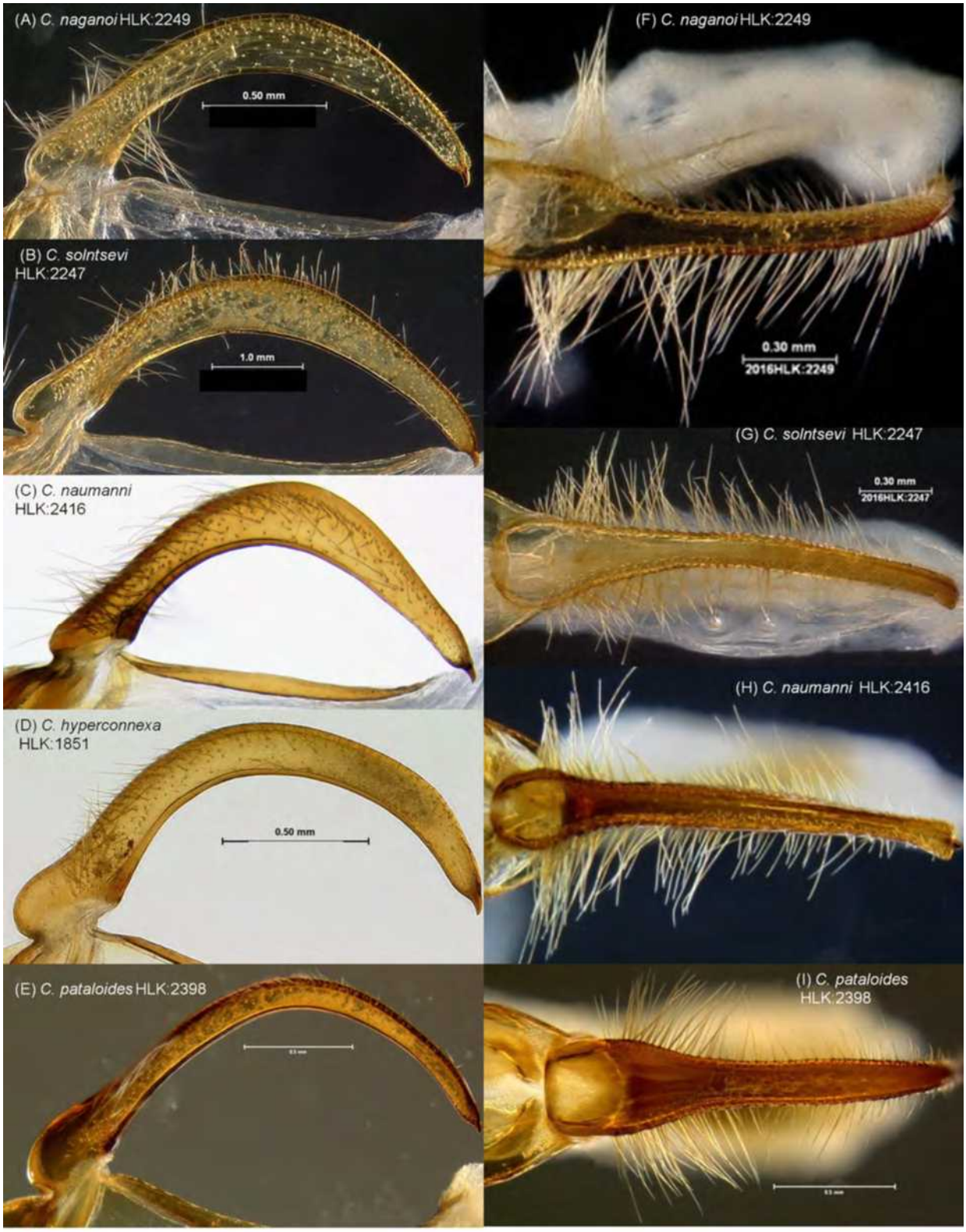

FIGURE 12. Comparison of the uncus between six *Catocala* species (left side: lateral aspect; right side: posterior aspect).

FIGURE 13. Comparison of the phallus and ductus ejaculatorius between six *Catocala* species: A–E & K: phallus with coecum opening lateral and on top; F–J: phallus with coecum opening face on; L–Q: ductus ejaculatorius.

COI 5': Three consistent character state differences were recorded between *C. katsumii* (n=3, all from type locality) and *C. naganoi* (n=1, plus 1 partial sequence): *C. katsumii* has 50 (T), 136 (C), and 343 (C), whereas *C. naganoi* has 50 (C), 136 (T), and 343 (T) (Table 1). States 50 (C), 136 (C), 343 (C), and 343 (T) are recorded from only one *C. naganoi* group species. The clade of *C. katsumii* + *C. naganoi* can be distinguished from all other sequenced *Catocala* by the following unique combination of character states: 28 (G), 40 (G), 88 (T), 235 (T), and 574 (C). All these states are unique to the *C. katsumii* + *C. naganoi* clade within the *C. naganoi* species group.

Catocala naumanni is diagnosed by the combination 241 (A), 289 (G), 364 (C), 400 (C), and 477 (A), and *C. solntsevi* is diagnosed by 180 (G), 265 (C), and 438 (C) (Fig. 16). Character states with black circles in Fig. 16 are unique to the specimens above their node among the specimens included in the analysis (all included in Fig. 16). All haplotypes recorded within the *C. naganoi* species group are presented in Table 1.

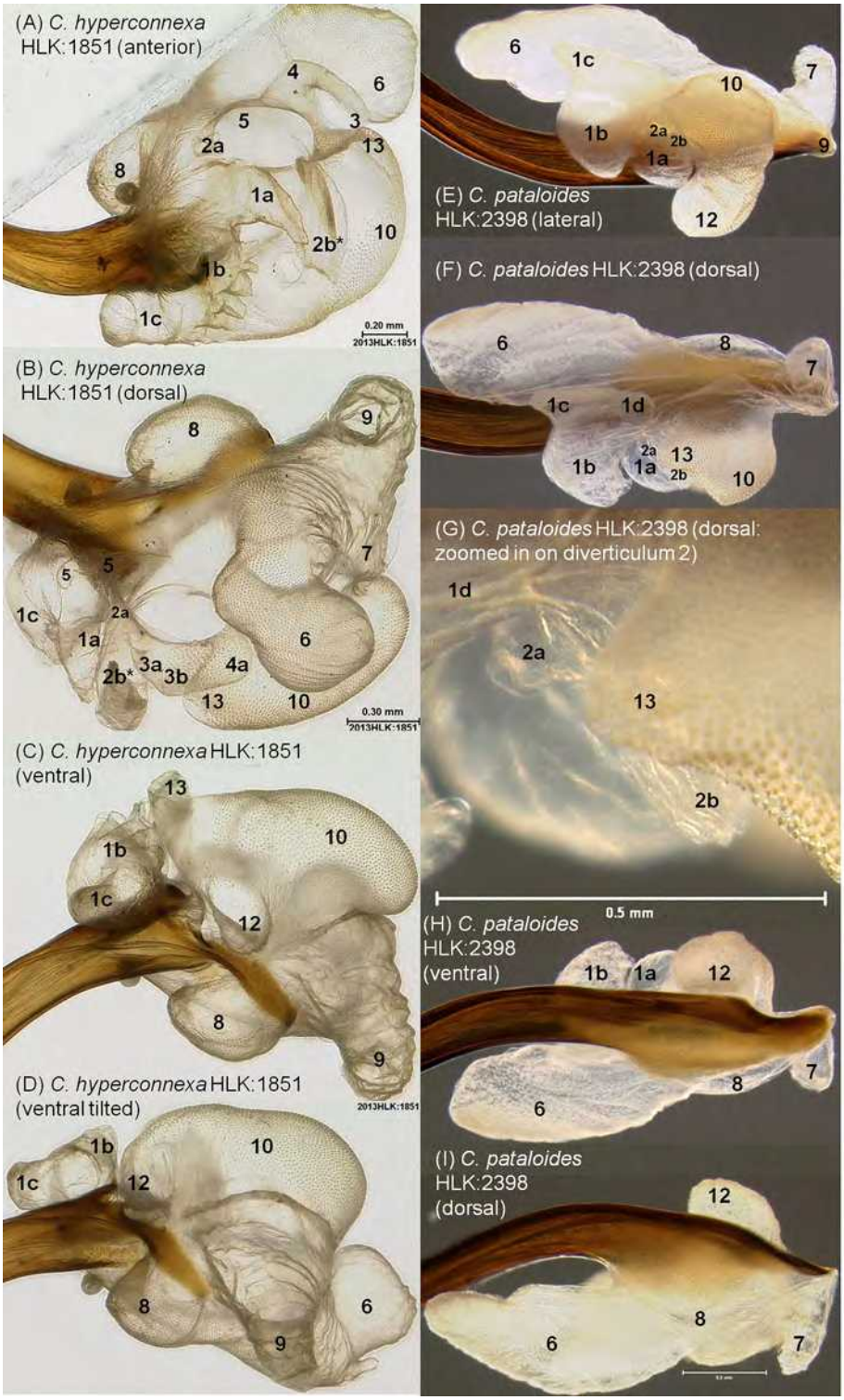

FIGURE 14. Three dimensional vesica structure for *C. hyperconnexa* and *C. pataloides.*

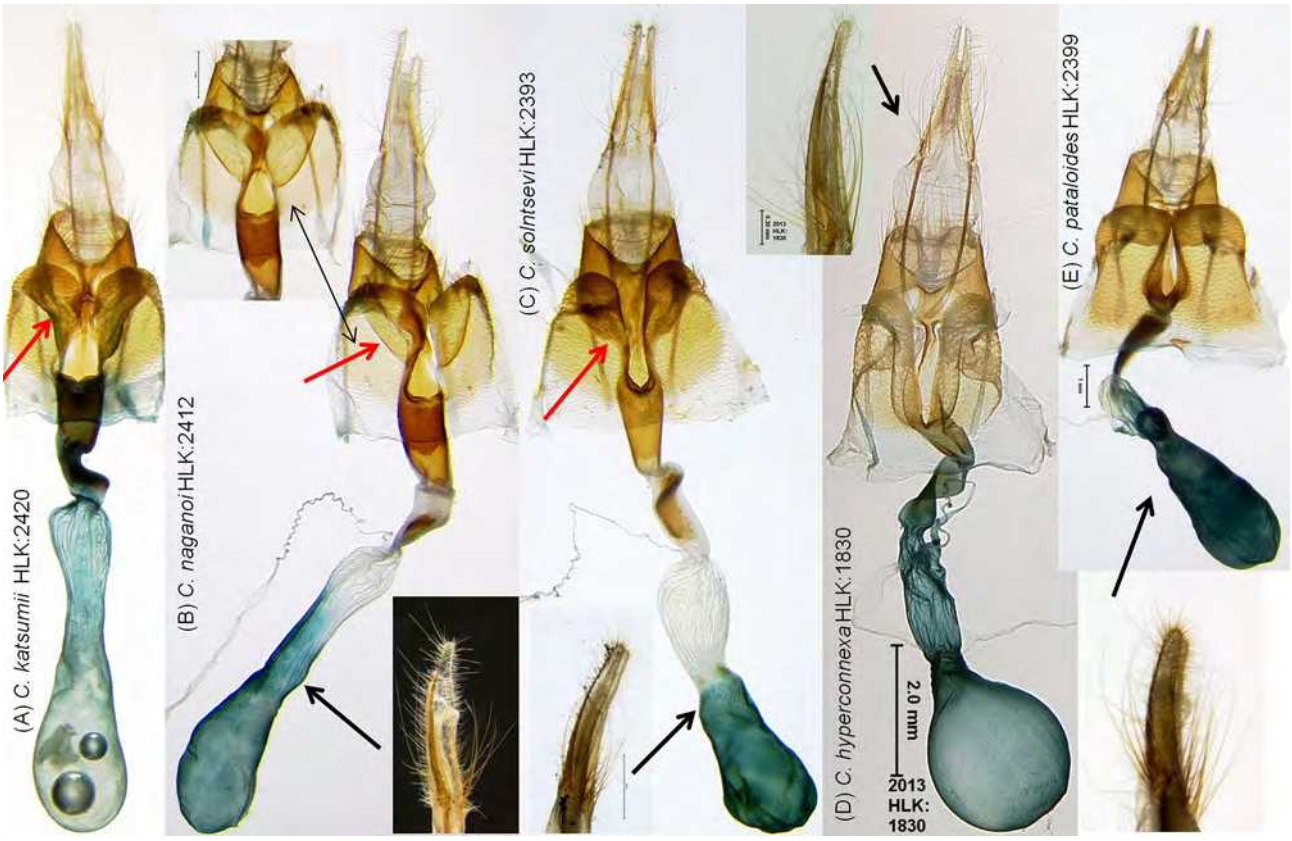

FIGURE 15. Comparison of female genitalia between five *Catocala* species (ventral habitus and lateral anal papillae; black arrows associate lateral anal papillae and ventral habitus photos).

TABLE 1. COI 5' haplotypes in the *C. naganoi* species group.

Character	28	40	50	88	127	136	160	217	220	235	241	265	271	274	289	325	328	337	343	364	400	436	457	477	574	607	625
Catocala naganoi 22032 Taiwan	G	G	**C**	T	T	T	A	A	T	T	T	T	C	C	A	T	A	A	**T**	T	T	T	T	G	C	T	A
Catocala naganoi 8035 Taiwan	G	G	**C**	T	T	T	A	A	T	T	T	T	C	C	A	?	?	?	?	?	?	?	?	?	?	?	?
Catocala katsumii 22027 Vietnam (type locality)	G	G	T	T	T	**C**	A	A	T	T	T	T	C	C	A	T	A	A	**C**	T	T	T	T	G	C	T	A
Catocala katsumii 22029 Vietnam (type locality)	G	G	T	T	T	**C**	A	A	T	T	T	T	C	C	A	T	A	A	**C**	T	T	T	T	G	C	T	A
Catocala katsumii 22030 Vietnam (type locality)	G	G	T	T	T	**C**	A	A	T	T	T	T	C	C	A	T	A	A	**C**	T	T	T	T	G	C	T	A
Catocala solntsevi 20376 Vietnam	A	A	T	**A**	T	T	**G**	A	T	C	T	**C**	C	C	A	A	A	A	A	T	T	**C**	T	G	T	C	A
Catocala solntsevi 20377 Vietnam	A	A	T	**A**	T	T	**G**	A	T	C	T	**C**	C	C	A	A	A	A	A	T	T	**C**	T	G	T	C	A
Catocala solntsevi 22043 Vietnam	A	A	T	**A**	T	T	**G**	A	T	C	T	**C**	C	C	A	A	A	A	A	T	T	**C**	T	G	T	C	A
Catocala solntsevi 1025 China	A	A	T	**A**	T	T	**G**	A	T	C	T	**C**	C	C	A	A	G	A	A	T	C	**C**	T	G	T	T	G
Catocala solntsevi 2131 China	A	A	T	**A**	T	T	**G**	G	T	C	T	**C**	C	C	A	A	G	A	A	T	C	**C**	T	G	T	T	G
Catocala naumanni 22033 China	A	A	T	C	C	T	A	A	C	C	**A**	T	C	C	**G**	A	A	A	A	**C**	C	T	T	**A**	T	T	A
Catocala naumanni 8065 China	A	A	T	C	C	T	A	A	C	C	**A**	T	C	C	**G**	A	A	A	A	**C**	C	T	T	**A**	T	T	A
Catocala kishidai 8085 Myanmar	A	A	T	C	C	T	A	A	C	C	T	T	**T**	**T**	A	A	A	**G**	A	T	T	T	**C**	G	T	T	A

Note: All COI 5' characters that vary within the *Catocala naganoi* species group are included. Character states unique to one species in this group appear in bold faced type.

Description. **Head.** Vertex with mixed brown, grey, and whitish scales. Frons with predominately brown scales medially and white bands laterally. Labial palp basal segment almost exclusively white, with sparse grey scales on the lateral side; middle segment with white band on basal, distal, and ventral sides, predominately dark grey elsewhere; terminal segment predominately dark grey, with scattered light grey and white scales. Antennae dorsally and laterally covered by grey scales, except for pedicel which is covered with white scales.

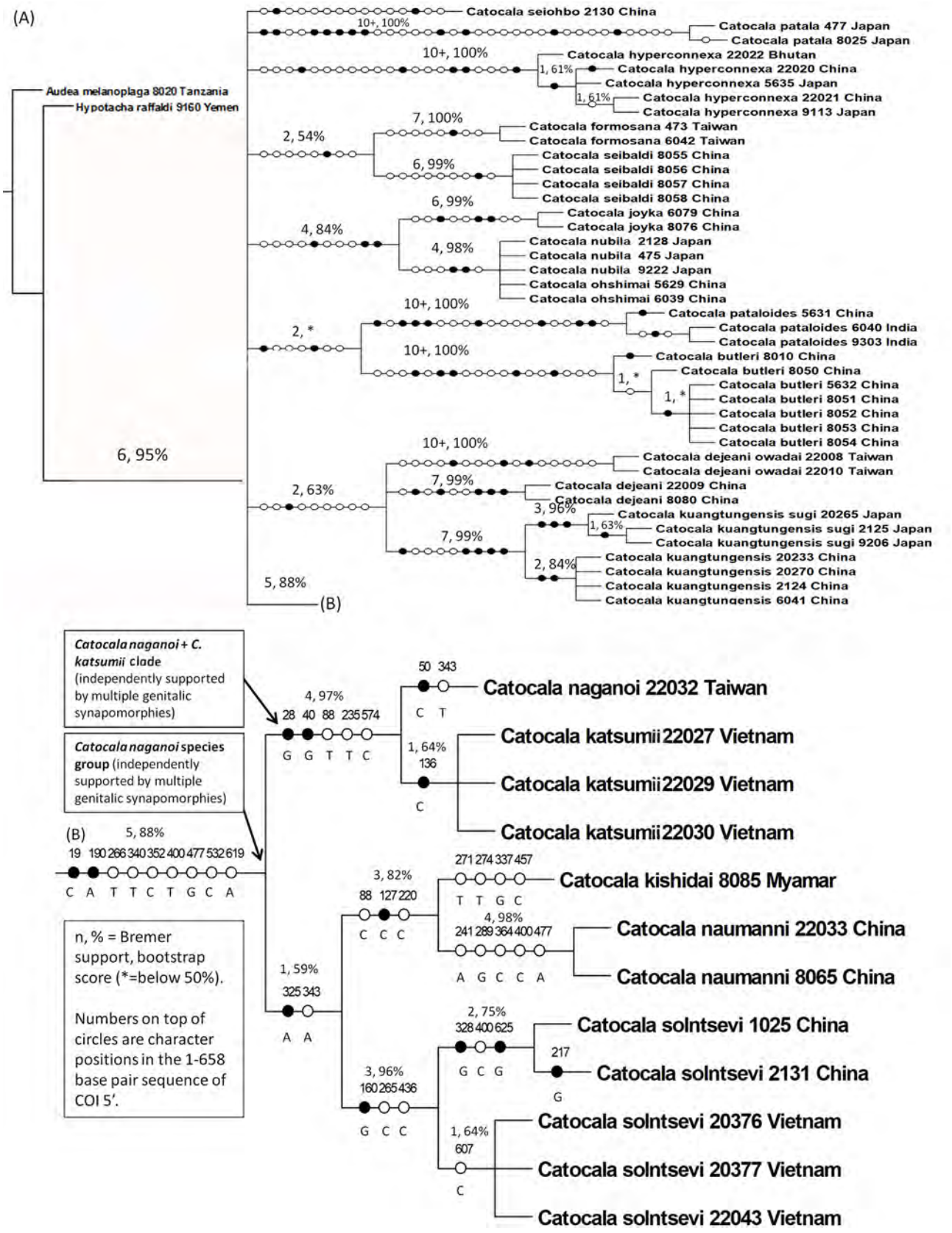

FIGURE 16. Diagnostic unique combinations of COI 5' characters for the *Catocala naganoi* species group and its constituent species. Diagnostic characters are mapped on the strict consensus of most parsimonious cladograms.

FIGURE 17. Ngoc Linh Mountain, the type locality of *C. katsumii* (photo by Vadim Golovizin).

Thorax. Patagia predominantly dark grey with transverse white bands and lighter grey with mixed white scales distally. Tegulae with mixed dark grey, light grey, brown, and whitish scales, without distinct bands. Elsewhere dorsally a mix of different shades of grey and brown scales and hairs with scattered white. Some whitish scales on thorax and tegulae with a bluish tint. Ventrally with dense whitish tan hairs.

Wings (Figs. 1: A–G). Length of anterior forewing base to apex: 25–29 mm males (n=9), 23–29 mm females (n=9); ratio of (anterior forewing base to apex)/ (anterior forewing base to tornal angle): 1.2–1.4 in both genders (wing shape not sexually dimorphic). Comparative forewing data: Males: *C. katsumi* (range=25–29 mm, mean=26.4, n=9); *C. naganoi* (range=30 mm, mean=30 mm, n=2); *C. solntsevi* (Vietnam: range=28–33 mm, mean=30.4 mm, n=25) (China: 33 mm, n=1); *C. hyperconnexa* (range=24–25 mm, mean=24.7 mm, n=4). Females: *C. katsumii* (range=23–29 mm, mean=26.2 mm, n=9); *C. naganoi* (range=26–29 mm, mean=28.0 mm, n=3); *C. solntsevi* (Vietnam: range=29–31mm, mean=30.3 mm, n=7); *C. hyperconnexa* (27 mm, n=1).

Forewing upperside (Figs. 1: A–C & E–F): Background color predominantly brown and grey with variable peppering of pale tan scales. Slightly denser brown scaling between postmedial and subterminal lines, and sometimes along basal sides of postmedial and antemedial lines. Basal dash present in both genders, short and thin, not extending distal of basal line, dark greyish–black, typically sharp with thin diffuse area around edges, occasionally diffuse throughout. Basal line sharp and black above cell CuA2, comprised of two loops, anterior loop fused with a black costal patch. Antemedial line single, comprised of five loops: posterior loop (below vein 2A) convex, thick and sharp contrasting black, margins more diffuse with black and dark brown; second (medial) loop large and convex spanning between veins 2A and lower margin of discal cell, of variable intensity but the most diffuse and least contrasting loop, comprised of brown or black and brown scales, sometimes medial section barely discernible from background (as in holotype); remaining loops thick and contrasting, comprised of dark brown or dark brown and black scales, midline regions sharp but edges may be diffuse; third loop convex, spanning posterior margin of discal cell to veinlet; fourth loop roughly triangular with apex near anterior margin of discal cell; fifth loop short and thick, convex, anterior to radial vein. Medial line double but limited to two black–dark brown patches between costa and the anterior margin of discal cell. Postmedial line of variable thickness, black; bordered distally by thin band of pale whitish grey to tan posterior of vein CuA2. Postmedial line undulations: below vein 2A convex, thick, mostly sharp but with more diffuse edges; between Cu2 and 2A single to weakly doubly dentate at apex; posterior side thickest part of postmedial line, anterior side thin, subreniform closed, connected to postmedial line by a single thin line; thin triangular tooth between veins Cu1 and Cu2; thicker but narrower triangular tooth between veins M3 and Cu1; two dentate distally protruding teeth between veins M1 and M3 with deep triangular division between them across vein M2, the tooth anterior to vein M2 extends slightly farther

distally than the tooth posterior to vein M2, apices and sometimes base of each tooth distinctly thickened; jagged and angling basally between veins R5 and M1, then sharply turned basally along vein R4, roughly perpendicular to costa, then thickened as a wide black patch slightly distal to the outer border of the reniform. Reniform spot closed with diffuse, double, brown to black border, diffuse brown scaling inside slightly contrasting with the more greyish median area. Subterminal line indistinct, a series of diffuse, light grey, dentate to undulate, distally protruding chevrons; one chevron between each pair of veins between R4 and 2A, half chevron between R4 and the costa, indistinct or half chevron between 2A and the inner margin. A diffuse dark brownish band sometimes present distal of the postmedial line between veins M2 and R5, slanting posteriorly outward to outer margin at vein R5. Wing margin with series of thin, diffuse, black to dark grey, concave bars between each pair of veins from R4 to 2A. Fringe peppered with variable shades of grey.

Hindwing upperside (Figs. 1: A–C & E–F): Background color orange–yellow throughout, no dark suffusion in hindwing background basal area inside or posterior to median band. Black median band sharp and thick, forming a complete loop with anterior and posterior sides converging at base of wing where only separated by a thin sliver of hindwing background color, distal side smooth to slightly angled along vein M2, both sides bulged between veins M2 and Cu1, band curved distally in cell CuA2, posterior side of loop thick along vein 2A. A dark band all along the inner margin paralleling the median band, but thinner, more diffused, and sometimes more greyish than the medial band. Posterior side of median band connected or nearly connected with inner marginal band by a diffuse black patch in the anal cell, positioned slightly basal to the farthest distal extent of the median band (between veins 2A and Cu2). Marginal black band thickest anteriorly, progressively narrowing posteriorly as far as vein M3, of fairly uniform thickness between veins M3 and Cu2, broken or narrow in cell CuA2, a wide patch at vein 2A, terminating before inner margin. Median and marginal bands doubly connected by black bands along veins Cu2 and 2A, the latter contiguous with the posterior side of the median band. Fringe orange–yellow, with black patches at ends of veins M1–Cu2, patches may be fused together between some veins; fringe black from the terminus of vein 2A to the inner margin. Apical patch wide with orange–yellow scales matching background color.

Forewing underside (Figs. 1: D & G): Background color pale yellow–orange. Marginal band thick and black, basal margin sharp, distal margin somewhat indistinct as area between marginal band and outer margin with dark grayish black only slightly lighter than the marginal band. Medial and basal bands wide and black, connected by an inner marginal band posterior of the veinlet between veins 2A and Cu2. Background color separates marginal and medial bands throughout their length, may be clean throughout or diffused with blackish scaling posterior of vein Cu1. Basal band thick and black, sharp posterior to discal cell, still predominately black with some diffusion of lighter tan scales anterior to lower margin of discal cell. Basal area with a small patch of background color. Fringe blackish.

Hindwing underside (Figs. 1: D & G): Background color pale orange–yellow like forewing. Medial black band of similar shape as dorsally but slightly thinner. Marginal black band of similar shape as dorsally, but relatively thicker across cell CuA2, and contiguous even if broken dorsally. Black band along inner margin much thinner and more diffuse than dorsally, not fused with median band. Median and marginal bands doubly connected by black bands along veins Cu2 and 2A, but connections narrower and more diffuse, more so along vein Cu2 than 2A. Fringe similar to upperside.

Legs (Figs. 3: O & V–AC (male)). Male and female legs similar with two exceptions: (1) male profemur with laterally flattened apical spine on dorsal corner (Fig. 3: O), (2) male mesotibia wider than female and with hair pencil groove on inner side (Fig. 3: X).

Foreleg (Figs. 3: O, V, & Z): Protibia unspined, but with small convex sulcus with radiating spines near basal extremity on the inner side (Fig. 3: V). Protibial flange in shallow ovuloid pit, ventral margin of flange with short row of setae (Fig. 3: V). Protarsomeres 1–4 with three ventral rows of large triangular spines, and two rows of minute hair–like curved spines between them (Fig. 3: AC); protarsomere 5 with four rows of large triangular spines, with two rows of minute hair–like spines in–between (Fig. 3: AA). Minute hair–like spines present on lateral sides of tarsomeres and along dorsal midline. Protarsomere 5 with pair of elongate, narrow, tubular spines dorsally at apex, then curving ventrally at apex. Pretarsus simple, arolium translucent and ovuloid with lateral sclerotized bands (Fig. 3: AA).

Midleg (Figs. 3: W–X, AA & AC): Mesotibia with a single row of seven heavily sclerotized large spines (Fig. 3: W). Tarsal spination like foreleg.

Hindleg (Figs. 3: Y & AB): Sclerotization pattern typical for *Catocala*, with femur sclerotized throughout,

metatibia translucent white except at base (Fig. 3: Y), metatarsomere 1 translucent white except at apex, remaining tarsomeres sclerotized throughout (Fig. 3: Y). Metafemur and metatibia unspined, metatarsal spination like foreleg.

Abdominal Scale Pattern. Dense brown colored scales dorsally over grey background, white, pale tan, and lighter grey scales ventrally.

Abdominal cuticle. Male as shown in Figs. 3: S–U. Female: Segments 1–6 similar to male, tergite 7 as shown in Fig. 5:G.

Male genitalia (Figs. 3: A–N & P–Q, 4: A–F, 6: A–B, 7: A, 8: A, 9: A–B, 10: A–B, 11: A, 13: A, F & L).

Capsule (Figs. 3: A–C): Juxta and vinculum strongly fused with valvae, vinculum weakly fused with tegumen, vinculum arms prominently expanded and weakly fused midventrally. Diaphragma membranous except for juxta/anellus, but weakly pigmented posterior of anellus.

Valvae (Figs. 3: E & J–K, 9: A–B, 10: A–B): Outer surfaces densely covered with elongate tan hairs and scales except for anterior portion of sacculus (Fig. 3: C), ventral half of "cucullus" (or the membranous valvae structure in the equivalent position) with dense elongate brown hairs/scales (Fig. 3: C); inner surface of cucullus with shorter scales and hairs along ventral margin (Fig. 3: C). Saccular process fused with band of ventral sclerotization on the anterior side of the cucullus (Figs. 9: A–B & 10: A–B); left saccular process narrow and elongate, over 4.5X as long as wide with a pointed posterior apex (Figs. 9: A–B); right saccular process thin and narrow, about 4X as long as wide with a curved and pointed apex (Figs. 10: A–B). On both valvae with inner side of sacculus with about 20 elongate setae near fusion with cucullus (Figs. 9: A–B & 10: A–B). Additional setae scattered along posterior margin of sacculus on inner side. Ventral inner sides of sacculus with concave indentation along margin of clasper base (Fig. 3: A). Left and right cucullus unpigmented except for ovoid patches of sclerotization bordering the ventral margin on the anterior side (Figs. 9: A–B & 10: A–B). Cucullus with scattered elongate setae on inner surface along ventral margin, densest anteriorly. Left costa heavily sclerotized, wide at base and tapering distally, of similar width for most of length with a slight medial expansion, then flared apically posterior to cucullus on the ventral side, posterior edge serrate, ventral corner bluntly pointed, dorsal corner convex (Figs. 9: A–B). Right costa dissimilar to left, wide and abruptly tapering distally at base, then progressively widening until terminating slightly distal of clasper apex but well anterior to posterior edge of cucullus, posterior edge indistinct, dorsal edge sharp and distinct, roughly semicircular subapical unpigmented area extending basally as a narrower band tapering to a point and paralleling the ventral side of the sharp costal margin (Figs. 10: A–B). Dorsally both costae fairly smooth along the length of the tegumen, distal to the sharp bend near base of uncus becoming slightly more irregular and undulated (Fig. 3: B). Claspers asymmetric (Figs. 3: A & E); both dorsoventrally flattened basally, fairly tubular distally. Left clasper (Fig. 3: J) in inner aspect ventral side concave; dorsal side irregularly undulated basally, concave distally; apex flared about 2X the medial width of the shaft, convex posteriorly and on sides, with about 25 scattered, minute, short setae, including 15 in a coplanar arc across the lateral edge; sparse, scattered short setae along clasper sides; patch of about ten elongate setae just anterior of the ventral side of clasper base. In ventral aspect projects ventrally inward, appearing fairly straight (Fig. 3: A). Right clasper (Fig. 3: K) in inner aspect ventral side concave; dorsal side convex basally and weekly concave medially–subapically; apex flared unevenly to over 2X the medial width of the shaft, ventral side more flared than dorsal side, flared area curved inward at apex, about 10–15 minute, short setae scattered around apex but none appearing in a coplanar arc along the edge; sparse, scattered minute setae on sides of shaft but no elongate setae. In ventral aspect irregularly projecting ventrally inward, shaft broadly curved ventrally, apex curved ventrally/inward at roughly a 90 degree angle (Fig. 3: A).

Juxta (Figs. 3: L & 11: A): Two elongate nearly symmetrical lobes, narrowest posteriorly, progressively widening anteriorly. Lobes broadly fused to anellus for over half the length of the posterior sides, touching at posterior end but not fused together. Pitted pattern of anellus not extending to juxta lobes at extreme posterior and posterior–outer edges.

Anellus (Figs. 3: L & 11: A): Lobes fused together throughout and appearing as a single sclerotized plate, highly asymmetrical. Left lobe (ventral aspect) broad and widening basally, then strongly curved and tapering to a narrow point distally; posterior side with a convex bulge basally, then deeply concave; anterior side strongly convex basally, broadly and shallowly concave distally. Right lobe over twice as wide as left lobe at widest point, widening for a short distance basally, then tapering to a narrow point distally, apex slightly curved posteriorly; posterior side convex basally, concave distally; anterior side convex basally, shallowly concave distally. Right lobe of anellus with a posterior translucent lightly scerotized membranous extension, base of this expansion including

about the posterior half of the inner side of the right lobe and a short distance around the posterior apex of the lobe. Left lobe with dense shallow depressions (pits) throughout, but less dense in a small ovuloid interior area adjacent the basal edge of the bend; right lobe with the pits around the entire margin of the lobe, but with a broad area in the interior of the wide basal section devoid of pits.

Uncus (Figs. 3: H–I): In lateral aspect (Fig. 3: I) widest medially, slightly widening from base to median area, progressively tapering and distinctly narrowing from medial area to apex; posterior side strongly convex, anterior side strongly concave. In posterior aspect widest subbasally, then narrowing and constricting before slightly widening medially and then tapering distally. Terminating in heavily sclerotized curved spine, laterally appearing pointed apically but narrowly rounded in dorsoventral view. Setae densest and longest at swollen base, longest setae over 1.6 X the maximum width of the uncus in posterior aspect (Fig. 3: H), dense nearly as long setae extend into medial area (clearest in posterior aspect), then abruptly shortening distal of the medial area and decreasing in density.

Tuba analis (Fig. 3: F): Membranous except for scaphium. Scaphium an elongate rectangular plate terminating slightly dorsally to the uncus apex.

Phallus (Figs. 3: G, M–N & P, 4: A, 13: A & F): Translucent throughout. Curved in three dimensions, cannot be viewed two dimensionally in any plane, apparent shape highly variable depending on orientation (Fig. 13: A versus F). Coecum shape clearest with opening orientated face on (Figs. 3: N & 13: F), posterior portion with a broad curve to the left, anterior apex with a weaker posterior curve. Shaft between coecum and hood doubly bent but bends occur in different planes and each are clearer in different orientations. With the coecum opening orientated face on, the first (anterior–most) bend is co–planar with the coecum; the shaft is curved to the left, such that the left side is convex and the right side is concave. The second bend curves ventrally and is clearest with the coecum opening viewed laterally and on top (Figs. 3: M & 13: A); this is the medial bend that is present in most *Catocala* species. Serrate band of small triangular teeth on the ventral side of the phallus posterior of the ventral bend, terminating posteriorly in a laterally flattened serrate keel reaching the base of the phallus hood (Fig. 3: P). Left flank of posterior ventral extension ("hood" over everted vesica) (Fig. 4: A) with a deep medial concave gouge (CG) and a convex expansions anterior and posterior of the gouge; right flank weakly convex, but appearing concave as the outer sclerotization is faint, and the boundary between lighter and darker sclerotization is concave; apex emarginate with two convex lobes divided medially by a concave gouge. Four sclerotized chords present on the ventral hood; inner chords (LIC and RIC) cross near base of the hood where they are prominent, then approximately parallel and much fainter throughout the length of the hood; right outer chord (ROC) prominent for over half the basal length of the hood, then abruptly becoming much fainter; right sclerotized plate (RSP) prominent, extending along entire right flank; left outer chord (LOC) disjunctive, discontinuous near base of hood, moderately distinct until convex posterior expansion.

Ductus ejaculatorius (Figs. 3: Q & 17: L): Slender region with distinct bend just before scoop–shaped region. Scoop shaped region had a S–shaped curve with a medial twist in both preparations (Fig. 3: Q), but the twist can be curved over 180 degrees to create the C–shaped curve typical of most *Catocala* (Fig. 13: L)*;* subsequently, the apex of the scoop crosses the apex of the slender region and broad overlaps with the base of the scoop (Fig. 13: L).

Vesica (Figs. 4: A–F, 6: A–B, 7: A & 8: A): Vesica diverticulum 1 trilobal: each lobe of similar width with 1a longer than and partially curved over the apex of 1b in anterior aspect (Figs. 6: A–B), 1b slightly longer than 1c (Figs. 4: A & 6: A–B); 1a arched and pointed with three convex lobes on outer side (anterior aspect, Figs. 6: A–B), 1b and 1c convex lobes (Figs. 4: A & 6: A–B). Diverticulum 2 bilobal: 2a a small convex lobe; 2b with broad tapering triangular base, then with a narrower tubular section following a sharp bend, apex greatly expanded and covered with minute inverted teeth (teeth limited to expanded area), expanded area with a distinct triangular gouge on inner side, slightly concave on the inner side distal to this gouge, convex on outer side (Figs. 6: A–B). Diverticulum 3 a simple convex bulge, covered with inverted teeth (Figs. 6: A–B). Diverticulum 4 a simple convex lobe narrower than 3, with sparser and scattered inverted teeth (Figs. 6: A–B). Diverticulum 5 prominent and elongate, outer side with two shallow but distinct lobes, apex and inner sides convex (Figs. 6: A–B). Diverticulum 6 large and broad, wider than high, densely covered with inverted teeth (Figs. 4: B & D). Diverticulum 7 narrower and much longer than 6, curved around about 180 degrees and arching over the dorsal surface of the vesica for roughly 2/3 of its length (Figs. 4: D & F). Diverticulum 8 thin and narrow, not extending around the distal edge of the phallus hood (Fig. 4: B). Diverticulum 9 distinctly bilobal, 9a a shallow convex bulge, 9b curved with the outer side much longer than inner side and a more narrowly rounded apex (Figs. 4: A & D). Diverticulum 10a broad

simple lobe, posterior portion densely covered with inverted teeth, teeth continue more sparsely anteriorly along outer margin (Fig. 4: D). Diverticulum 11 not discernible. Diverticulum 12 a simple convex lobe with apex extending ventrally over the left side of the phallus hood, densely covered with inverted teeth (Figs. 4: A–B). Diverticulum 13 a prominent fang–shaped lobe, with scattered inverted teeth along outer edge (Fig. 4: C). Vesica unpigmented throughout (Fig. 4).

Female genitalia (Figs. 5: A–K & 15: A) (n=2).

Papillae analis (Figs. 5: A–B, H, & J): Transparent except for a thin band of dorsal sclerotization on each papilla, terminating subapically. Longest setae at base, projecting posterior/outward. Shorter setae throughout papillae project posterior/outward. Apices densely covered with setae of highly variable lengths (Figs. 5: H & J). Papillae curved such that dorsal side strongly convex and ventral side weakly and doubly concave, but with small convex area at base (Fig. 5: J). Papillae widest at base and gradually tapering but with a slight subapical widening, narrowest apically (Fig. 5: J).

Intersegmental membrane between papillae and segment 8 (Figs. 5: A–B & 15: A): Bulging out with sides convex, posterior end nearly as wide as anterior end, widest medially. Ratio of length to width at anterior end = 1.7–1.8.

Segment A8 (Fig. 5: B): Anterior edge of sides overlapping with posterior edge of lamella antevaginalis. Shape as shown in Fig. 5: B. Elongate, posteriorly projecting setae scattered throughout sclerotized surfaces, greatest density posteriorly along edge.

Intersegmental membrane between lamella and segment 8 on ventral side (Figs. 5: A & F): Heavily sclerotized with three differently shaped sections; posterior section triangular and tapering anteriorly; medial section roughly diamond–shaped, contrastingly heavily sclerotized band on sides contiguous along posterior edge, but noncontiguous on anterior edge; anterior section inverted U–shaped, widening anteriorly, longitudinal sclerotized band along midline. Posterior and medial sections densely covered with minute spiculations, spiculations in anterior section limited to the posterior portion of the sclerotized midline band.

Lamella antevaginalis (LAV) (Figs. 5: A & 15:A): Sides bent dorsally, somewhat asymmetrical, appearing less asymetrical if sides flattened out, but thicker where connected to antrum on the left side (ventral aspect) than the right side. Posterior margins convex; anterior margins convex for a short distance beyond fusion with antrum but concave for remainder of length, not contiguous along dorsal midline, rather disjunct and not connecting across antrum. Slit in LAV along ventral midline wide and progressively widening anteriorly to the full width of the antrum at anterior terminus, sides slightly thickened at anterior margin.

Antrum (Figs. 5: A–C & 15: A): Sclerotized throughout. Sides convex, widest at anterior end of slit in LAV, gradually tapering anterior to this position and more strongly tapering posteriorly.

Ductus bursae (Figures 5: A–C & 15: A): Rectangular and strongly dorso–ventrally flattened with a sclerotized plate on each side, curved ventrally and to the right. Sclerotization variable, partially unsclerotized, in one preparation sclerotization limited to the ventral anterior edge, in the other preparation sclerotization widest at anterior edge, then tapering posteriorly but extending as far as the antrum.

Corpus bursae (Figs. 5: A–C & 15: A): Posterior section with longitudinal wrinkles elongate, about 3.5–4 X as long as wide at anterior base (ventral aspect), widening posteriorly, widest point slightly anterior to junction with ductus bursae. Anterior section densely covered with minute inverted teeth, vertically ovoid.

Ductus seminalis (Fig. 5: K): Total length approximately 12.5 mm. Section between corpus bursae and bula seminalis about 6.4 mm, coiled portion of this section with 6–8 coils and about fourteen inflexion points. Thicker fairly straight section distal to bulla seminalis about 3.0 mm.

Colleterial gland complex (Figs. 5: D–E & I): Terminology follows Mitter (1987). Adjoining differentiated canals of receptacle duct with three coils basal to the vesicle; abrupt transition to undifferentiated section at base of vesicle; vesicle sclerotized, comma shaped, thinner than preceding coils (Fig. 5: E). Utriculus elongate with many narrow longitudinal grooves throughout (Fig. 5: I). Lagena with two distinct sections, base narrow and tubular and progressively but slightly widening distally, distal section abruptly, progressively, and strongly widening, somewhat fan–shaped with an irregularly but somewhat flattened apical margin (in contrast to the ovoid shape typical of most *Catocala* species) (Fig. 5: I). Colleterial gland narrowest at base and irregularly widening distally, curved and asymmetric, the sack from which the paired glands arise not clearly differentiated from stalk (Fig. 5: D). Oviductus communalis with simple section about twice as long as paired section (Fig. 5: D). Vagina ovoid (Fig. 5: D).

Rectum/Intestine. Rectum sculptured throughout with small ovuloid shapes with slightly raised walls. Male intestine thin, as shown in Fig. 3: R.

COI 5' Mitochondrial DNA: All three sequenced specimens of *C. katsumii* have the following haplotype for positions 1 to 658:

AACTTTATATTTTATTTTCGGAATTTGGGCAGGAATAGTGGGAACTTCATTAAGATTATTAATTCGAGCT
GAATTAGGTAATCCTGGTTCTTTAATTGGAGATGATCAAATTTATAATACTATTGTTACAGCTCACGCTT
TTATTATAATTTTTTTTATAGTTATACCAATTATAATTGGAGGATTTGGAAATTGATTAGTACCTTTAATAT
TAGGAGCTCCTGATATAGCTTTTCCTCGTATAAATAATATAAGTTTTTGACTTTTACCCCCCTCATTAACT
TTATTAATTTCAAGAAGAATTGTAGAAAATGGAGCAGGAACTGGATGAACAGTATATCCCCCTCTTTCC
TCTAATATTGCTCATAGAGGTAGTTCAGTAGATTTAGCTATTTTTTCTTTACATTTAGCTGGAATTTCTTC
AATTTTAGGAGCTATTAATTTTATTACTACAATTATTAATATACGATTAAATAGTTTAATATTTGATCAAAT
ACCTTTATTTATTTGAGCTGTAGGAATTACTGCATTCCTTCTTCTTCTCTCATTACCAGTATTAGCTGGAG
CTATTACCATACTTTTAACTGATCGAAATTTAAATACTTCTTTCTTTGATCCAGCTGGAGGAGGAGATCC
TATTTTATATCAACATTTATTT

Etymology. The new species is named for Katsumi Ishizuka, who has devoted many years to advancing the understanding of *Catocala*.

Biology and distribution. *Catocala katsumii* appears to be endemic to the Indochinese Peninsula. All but one of the specimens have been taken at the type locality of Ngoc Linh Mountain in the Central Highlands of Vietnam at 1700 m (Fig. 17; the other specimen was taken at 1600 m in the northwestern mountainous region of Vietnam adjacent to Yunnan, China). *Catocala solntsevi, C. pataloides* and *Ulotrichopus macula* (Hampson, 1891) occur with *C. katsumii* at the type locality. The larval hosts of *C. katsumii* and other species in the *C. naganoi* species group are unknown. The recorded phenology for *C. katsumii* is unusual among *Catocala* species, with fresh specimens recorded from May, June, July, October, and December. In the Nearctic, some larger *Catocala* species have a nearly comparably extended flight season, but fresh specimens predominate in the summer months.

On Ngoc Linh Mountain, Sino–Himalayan (Juglandaceae, Ulmaceae, Lauraceae) and Malesian (Myrtaceae, Sterculiaceae) tree families are intermixed and present at all altitudes. Above 1000 m. typical Vietnamese medium montane broad–leaved evergreen forest becomes increasingly dominant, with Sino–Himalayan floral elements (Fagaceae, Lauraceae, Magnoliaceae) and some conifers mixed in, and disturbance levels are lower and precipitation is heavier (>3500 mm annually; Hurley 2001). High lepidopteran diversity in Vietnam is in part due to changes in topography and climate patterns with links to adjacent Sino–Himalayan, Sundanian and Indo–Burmese faunas, with the Kon Tum plateau alone having 16 endemic butterfly species (including 9 of Indo–Burmese origin; Monastyrskii and Holloway, 2013). The newly described *Catocala becheri* Borth, Kons, & Saldaitis, 2017 also appears to be endemic to the Central Highlands.

Remarks.

Catocala naganoi Sugi, 1982

(Figs. 1: H–L, 5: L, 6: C, D, 7: C, D, 8: C, D, 9: C, D, 10: C, D, 11: B, C, 12: A, F, 13: B, G, M & P, 15: B)

Catocala naganoi Sugi, 1982, *Tyo to Ga*, 32(3–4), 147–159, (TL: Taiwan, Taoyuan Hsien [HT: coll. NSMT, Tokyo).

This species appears to be endemic to Taiwan, where it is recorded from Taoyuan (Fig 1: H & K–L) and Hsinchu Counties (Figure 1: I–J). The holotype of *C. naganoi* (Sugi 1982, Fig. 5) is typical in wing pattern to material we studied, and the valvae (Sugi 1982, Fig. 12) are similar to our dissections except for the left clasper, which appears to have been damaged and bent by ca. 180 degrees as a result of slide mounting.

***Catocala solntsevi* Sviridov, 1997**
(Figs. 1: M–R, 2: A–C, 5: M, 6: F–H, 7: E, F, 8: E, F, 9: F–H, 10: F–H, 11: D, E, 12: B, G, 13: D, E, N & O, 15: C)

Catocala solntsevi Sviridov, 1997, *Russian Journal of Zoology*, 76(6), 763–765, (TL : North Vietnam, Tam Dao [HT: coll. Zoological Museum of Moscow University).

This species is recorded from South China (Guangdong, Hunan and Guizhou Provinces) and Vietnam (Kon Tum, Quàng Nam, Thừa Thiên–Huế, Lâm Đồng Provinces and Da Nang Municipality). The male holotype (Sviridov & Korb, 2010, Fig. 16) exhibits the forewing phenotype with a whitish medial area, similar to Fig. 1:Q. Drawings of the holotype valvae and phallus (Sviridov, 1997, Fig. 1) are consistent with our dissections, including the tapering costal apex of the left valve, in contrast to the flared costal apex of all of the other *C. naganoi* group species. However, Sviridov's (1997, Fig. 1) drawing of the left anellus plate differs from our dissections by lacking an abrupt tapering and elongate, narrow terminus, and we suspect this difference is an artifact of limitations of the type drawing or dissection (note that care is needed during dissection to recover intact the fragile termini of the anellar plates when separating the anellus/juxta from the valvae).

Sequenced specimens of *C. solntsevi* from China and Vietnam form separate clades with four consistent COI 5' character state differences, but we found these to be indistinguishable by both external pattern and male genitalic morphology. In contrast, *C. katsumii* and *C. naganoi* have three consistent COI 5' character state differences, yet have numerous genitalic differences as elaborated above. This is yet another cautionary example of why degree of divergence in COI 5' sequences can be problematic when making species–level decisions, even within a group of closely related species.

***Catocala naumanni* Sviridov, 1996**
(Figs. 2: D–I, 6: E, 7: B, F, 8: B, 9: E, 10: E, 11: F, 12: C, H, 13: C, H)

Catocala naumanni Sviridov, 1996, *Journal of the Ukraine Entomological Society*, 2(3–4), 23–26, (TL : China, Yünnan, Li–kiang [HT: coll. ZFMK).

All known specimens were collected in close proximity to the type locality in northern Yunnan Province, China, at altitudes above 2000 m, and allopatric with the other members of the *C. naganoi* species group. Sviridov's (1996) published male genitalic drawings of the holotype show some marked differences from the preparations we examined (e.g., in the drawing, the left valva clasper parallels the dorsal edge of the costa and the phallus lacks a distinctive quadrate tooth). However, actual photos of the *C. naumanni* holotype genitalia differ from these drawings, and the features match our other preparations.

It is not clear that *C. solntsevi* and *C. naumanni* are separable by wing pattern alone, and we found no consistent differences in the limited series we studied. All recently collected *C. naumanni* examined (3 males, one female) have a dorsal forewing marginal shade posterior of vein 2A, which continues between the antemedial and postmedial lines, although it may be not as dark in this area (Figs. 2: D–H). In some specimens of *C. solntsevi* the marginal shade is relatively lighter between the antemedial and postmedial lines (Figs. 1: Q–R), or the darkest area is limited to the vicinity of vein 2A but not extending to the anal margin (Figs. 1: M & O–P). All specimens of *C. naumanni* examined (n=5) have the dorsal hindwing marginal band clearly unbroken in cell CuA2; three specimens examined of *C. solntsevi* (n=31) match these (Fig. 1: R), but the remainder either have the band broken or more narrowly joined in cell CuA2. However, the range of variation in this feature observed in *C. solntsevi* is typical of infraspecific variation in many *Catocala* species, and longer series of both species may be needed to circumscribe the patterns more crisply.

Acknowledgements

Larry Gall, Kyle Johnson, Hugo Kons, Sr., Sharon Kons, and David Wahl have supported our *Catocala* research in numerous ways. David Wahl and the former American Entomological Institute provided use of a GT Vision

imaging system, and Daniel Young and Kyle Johnson arranged use of an Auto–Montage imaging system at the University of Wisconsin–Madison. James Hayden, Katsumi Ishizuka, and Andre Sourakov loaned critical material for study. Adult and male genitalia images of the male holotype of *C. naumanni* were provided by Dieter Stüning. Katsumi Ishizuka and Alessandro Floriani provided corresponding adult and genitalia images for specimens of *C. naumanni, C. solntsevi* and *C. naganoi*. Vadim Golovizin contributed the type locality image. Thanh Lunog Le, John Heppner, Katsumi Ishizuka, Mamoru Owada, Andre Sourakov, and Hsiau–Yue Wang collected *C. naganoi* group specimens used in this study. Thanh Lunog Le supplied field notes from where he collected *C. katsumii* specimens. Paul Hebert's BOLD (Barcode of Life Data Systems) lab at the University of Guelph sequenced COI 5' for our *Catocala* samples. Mary Blair provided the citation for the Center for Biodiversity and Conservation at the American Museum of Natural History. Larry Gall and two anonymous reviewers provided a helpful review of this manuscript.

References

Borth, R. J., Kons Jr., H. L. & Saldaitis, A. (2017) A new species of *Catocala* (Lepidoptera: Noctuidae) from Vietnam. *Bulletin of the Peabody Museum of Natural History,* 58 (1), 47–64. https://doi.org/10.3374/014.058.0104

Butler, A.G. (1881) Lepidoptera Heterocera from Northern China, Japan, and Corea. *Transactions of The Royal Entomological Society of London,* (48) 534.

Goloboff, P.A., Farris, J.S. & Nixon, K.C. (2008) TNT, a free program for phylogenetic analysis. *Cladistics*, 24, 1–13. https://doi.org/10.1111/j.1096-0031.2008.00217.x

Felder & Rogenhofer (1874) Reise ost. Freg. Novara (Zool.)2 (2), Taf. 112:23.

Hampson, G.F. (1891) *Illustrations of Typical Specimens of Lepidoptera Heterocera in Collection of the British Museum. Part VIII*. The Lepidoptera Heterocera of the Nilgiri District, Taylor and Francis, London, 144 pp.

Hebert, P.D.N., Cywinska, A., Ball, S.L. & Waard, de J.R. (2003) Biological identifications through DNA barcodes. *Proceedings of the Royal Society B*, 270, 313–321. http://dx.doi /10.1098/rspb.2002.2218

Hurley, M.M. (2001) Multi–taxa biotic Inventories of three unprotected forested ecosystems in Vietnam. Retrieved 28 April 2017 from: *the Center for Biodiversity and Conservation at the American Museum of Natural History, New York, USA.* http://www.amnh.org/our-research/center-for-biodiversity-conservation/research-and-conservation/biodiversity-exploration-and-monitoring/past-projects/mainland-southeast-asia (Accessed 27 Nov. 2017)

Ishizuka, K. (2006) A new species of *Catocala* Schrank, 1802 from northern Sichuan, China (Lepidoptera Noctuidae) Tinea, 19 (2), 126–128.

Ishizuka, K. (2009) Records of four species of *Catocala* Schrank, 1802 (Lepidoptera, Noctuidae) including a new species from Burma. *Gekkan–Mushi*, 461, 53–55.

Kons Jr., H.L. & Borth, R.J. (2015) A new species of *Catocala* (Lepidoptera: Noctuidae) from the southeastern United States. *Bulletin of the Peabody Museum of Natural History,* 56 (1), 55–65.

Leech, J.H. (1900) Lepidoptera Heterocera from Northern China, Japan, and Corea. *Transactions of The Royal Entomological Society of London*, (48) 534. https://doi.org/10.1111/j.1365-2311.1900.tb02720.x

Madison, W. & Madison, D. (2011) *Mesquite: a modular system for evolutionary analysis*. Version 2.75. Available from: http://mesquiteproject.org

Mell, R. (1931) Zur Kenntnis südchinesischer Catocalinen (s. str.) (Lep.). *Mitteilungen der Deutschen Entomologischen Gesellschaft*, 2, 85–91. https://doi.org/10.1002/mmnd.4820020605

Mell, R. (1936) Beiträge zur Fauna sinica XI. Zur Biologie und Systematik der chinesischen *Catocala* (Lep. Heter.). Dt. ent. Z. Iris, 50, 49–90. [pl. 3.]

Mitter, C. (1987) Taxonomic potential of some internal reproductive structures in *Catocala* (Lepidoptera: Noctuidae) and related genera. *Annals of the Entomological Society of America,* 81, 10–18. https://doi.org/10.1093/aesa/81.1.10

Monastyrski, A.L. & Holloway, J.D. (2013) *The Biogeography of the Butterfly Fauna of Vietnam with a Focus on the Endemic Species (Lepidoptera).* Chapter 5 of Biochemistry, Genetics and Molecular Biology "Current Progress in Biological Research."

Nixon, K. (2002) *WinClada Software*. Published by the author, Ithaca, New York. Available from: http://www.cladistics.com/aboutWinc.htm (Accessed 27 Nov. 2017)

Okano, M. (1958) New or little known moths from Formosa (1). Ann. Rep. Gakugei Fac. Iwate Univ., 13(2): 51-56, pls. 1-2.

Sugi, S. (1965) New and unrecorded species of *Catocala* Ochs. from Japan and Formosa (Lepidoptera, Noctuidae). *Tinea*, 7, 84–93.

Sugi, S. (1965) New and unrecorded species of Catocala OCHS. from Japan and Formosa (Lepidoptera, Noctuidae). Tinea, 7, 84–93. [pl. 17.]
Sugi, S. (1982) Illustrations of the Taiwanese *Catocala*, with descriptions of two new species, Noctuidae of Taiwan 1 (Lepidoptera). *Tyo to Ga*, 32 (3–4), 147–159.
Sviridov, A.V. (1996) A new species of the genus *Catocala* (Lepidoptera, Noctuidae) from southern China. *Journal of the Ukraine Entomological Society*, 2 (3–4), 23–26.
Sviridov, A.V. (1997) A new species of the genus *Catocala* (Lepidoptera, Noctuidae) from North Vietnam. *Russian Journal of Zoology*, 76 (6), 763–765.
Sviridov, A.V. & Korb, S.K. (2010) An illustrated catalogue of primary type specimens of the Lepidoptera in collection of the Zoological Museum of Moscow State University described in the second half of XXth century. *Eversmannia*, 21–22, 6–27.